ACS OMEGA

http://pubs.acs.org/journal/acsodf

Mini-Review

"Smart" Polymer Nanogels as Pharmaceutical Carriers: A Versatile Platform for Programmed Delivery and Diagnostics

Namitha K. Preman,[†] Supriya Jain,[†] and Renjith P. Johnson*

Cite This: *ACS Omega* 2021, 6, 5075−5090

Read Online

ACCESS | Metrics & More | Article Recommendations

ABSTRACT: "Smart" polymeric nanoformulations are evolving as a promising therapeutic, diagnostic paradigm. The polymeric nanovehicles demonstrated excellent capability to encapsulate theranostic cargos and their successful delivery in physiological conditions and even to monitor the therapeutic response. Currently, polymer nanogels (NGs) are established as capable carriers toward triggered delivery of diverse therapeutic and diagnostic agents. Notably, biodegradable and "intelligent" NGs constructed from intelligent polymers are highly beneficial because of their responsiveness toward endogenous as well as exogenous stimuli like pH gradients, bioresponsiveness, photoresponsiveness, temperature, and so on. In the past decade, plenty of multifunctional NGs with excellent targetability and sensitivity were reported for a wide range of theragnostic applications. This mini-review briefly propounds the synthesis strategies of "smart" NGs and summarizes the notable applications like delivery of genetic materials, anticancer agents, photodynamic/photothermal therapies, imaging, and biosensing. Herein, we have also addressed the current clinical status of NGs and the major challenges that are essential to overcome for the further advancement of NGs for specific applications.

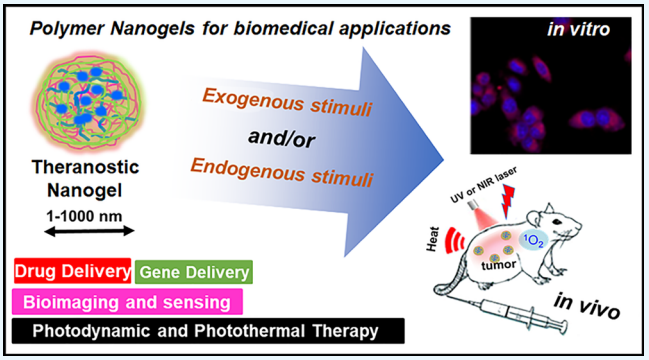

1. INTRODUCTION

Polymer nanogels (NGs) are aqueous dispersions of nanosized hydrogel particles, which usually formed through physical or chemical cross-linking of polymer chains which simultaneously demonstrate the features of hydrogels and nanoparticles. The NGs are three-dimensional nanonetwork structures and can be fabricated from a variety of synthetic or natural polymers and a blend thereof.[1] The NGs possess excellent ability to retain water without degrading into an aqueous medium, and features like size, surface charge, and the extent of degradation are customizable through changing polymer compositions. Usually, the NGs are spherical assemblies; however, the recent development in macromolecular engineering now allows the fabrication of NGs with diverse morphologies.[2] Based on the morphology and structural characteristics, NGs can be mainly categorized as core−shell, hollow, layer-by-layer (LBL), hairy, functionalized, and hybrid (Figure 1B).[3]

The NGs with core−shell morphology composed of chemically linked compartments and, in this category, the backfolding of cross-linked chains were restricted, and their fabrication is critical since it highly depends upon diverse parameters like size, core−shell density, and functional group modification, etc.[3] The hollow NGs are generally synthesized by thermoresponsive polymers. These NGs with cross-linked shell will show discrete temperature responsiveness and may not always be hollow due to the lack of void; however, NGs with a rigid shell will be hollow with reduced temperature responsiveness.[4] The LBL NGs are also cross-linked, and multilayers were fabricated in different dimensions with the aid of templates such as microgels, NGs, and even rigid particles.[3] The hairy NGs are a dual core−shell construct, and the shell consists of linear polymers of excellent dispersion capability and a core generally composed of inorganic or polymeric materials. The functionalized NGs were most common and were developed to enhance the stability of LBL NGs; however, extensive synthesis and purification steps are required.[3] The hybrid or composite NGs are referred to as the NG composed of inorganic polymers and/or with carbon-derived nanoassemblies, plasmonic and magnetic nanoparticles, and several others.[5]

Regardless of the structural differentiation, the above-mentioned polymer NGs can be classified under stimuli-responsive or "smart" polymeric nanovehicles and were engineered from different stimuli-responsive polymers to undergo a conformational or structural change according to

Received: October 29, 2020
Accepted: February 4, 2021
Published: February 15, 2021

https://dx.doi.org/10.1021/acsomega.0c05276
ACS Omega 2021, 6, 5075−5090

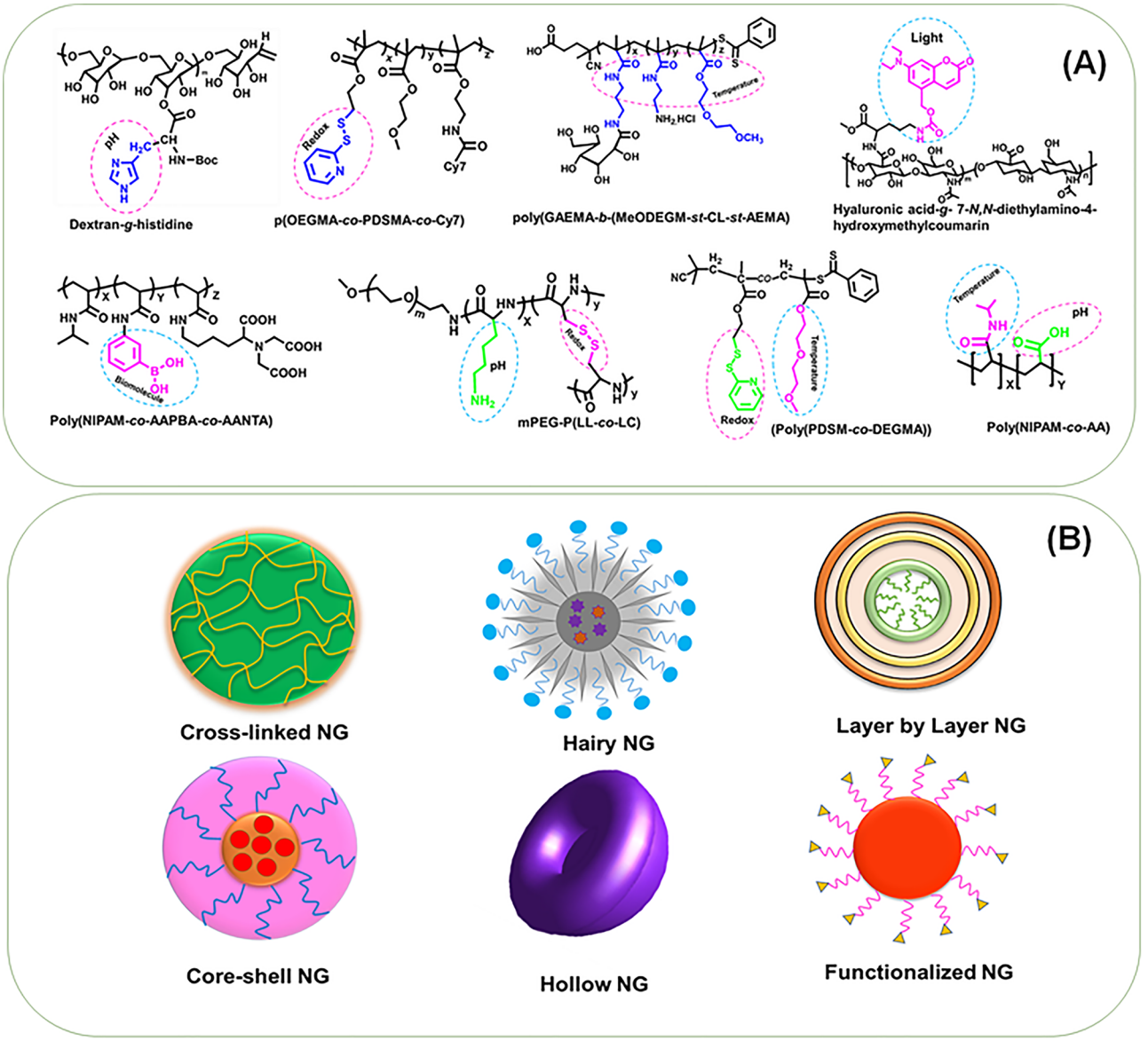

Figure 1. (A) Illustration of representative stimuli-responsive nanogel architectures. The responsive functionality and the corresponding stimuli response are highlighted in each structure. (B) The classification of stimuli-responsive nanogels based on their morphology and structural characteristics.

the variations of ambient conditions, toward an exogenous stimuli trigger (temperature, light, magnetic field) or an endogenous biological trigger (pH, bioreduction, biomolecule recognition, etc.). Representative NG architectures and their responsive moieties were highlighted in Figure 1A. Precisely, due to a stimuli trigger, the extent of disassembly of the NG network and the interaction with aqueous media typically result in either swelling or deswelling of the NG and subsequent release of the entrapped therapeutic/theranostic cargo. In pharmaceutical domains, "smart" NGs offer several other advantages, including hydrophilicity, enhanced water absorptivity, biocompatibility, and degradability, and the small size and capability for the active or passive targeting of a desired biophase or disease conditions. To date, a series of stimuli-responsive, biodegradable polymer NGs have emerged, and substantial advancement has been made especially for triggered delivery of drugs, nucleic acids, and imaging applications.[6−9] The polymer NGs were also successfully employed in the delivery of therapeutic oligonucleotides and protein drugs and even for combinatorial delivery therapeutics in treatment and diagnosis.[2] Notably, NGs demonstrated their versatility in fabricating magnetic resonance (MR) and positron emission tomography (PET), multimodal optical imaging formulation, and their successful applications.[5]

Polymeric nanostructures such as nanospheres, vesicles, micelles, dendrimers, etc. demonstrated wide structural options with functionalization flexibility for programmed delivery of theranostic agents. However, for a macromolecular nanodelivery system, it is crucial to maintain the biocompatibility and stability under physiological conditions. In this regard, compared to the conventional polymeric nanostructures, ideally designed NGs, with their unique size (1−1000 nm) as well as physicochemical characteristics, were highly stable. The NGs can exist in blood circulation for prolonged time and accumulate in targeted tissues to release the encapsulated theranostic cargo in response to various physiological stimuli.[9] The stability of the nanosystem

https://dx.doi.org/10.1021/acsomega.0c05276
ACS Omega 2021, 6, 5075−5090

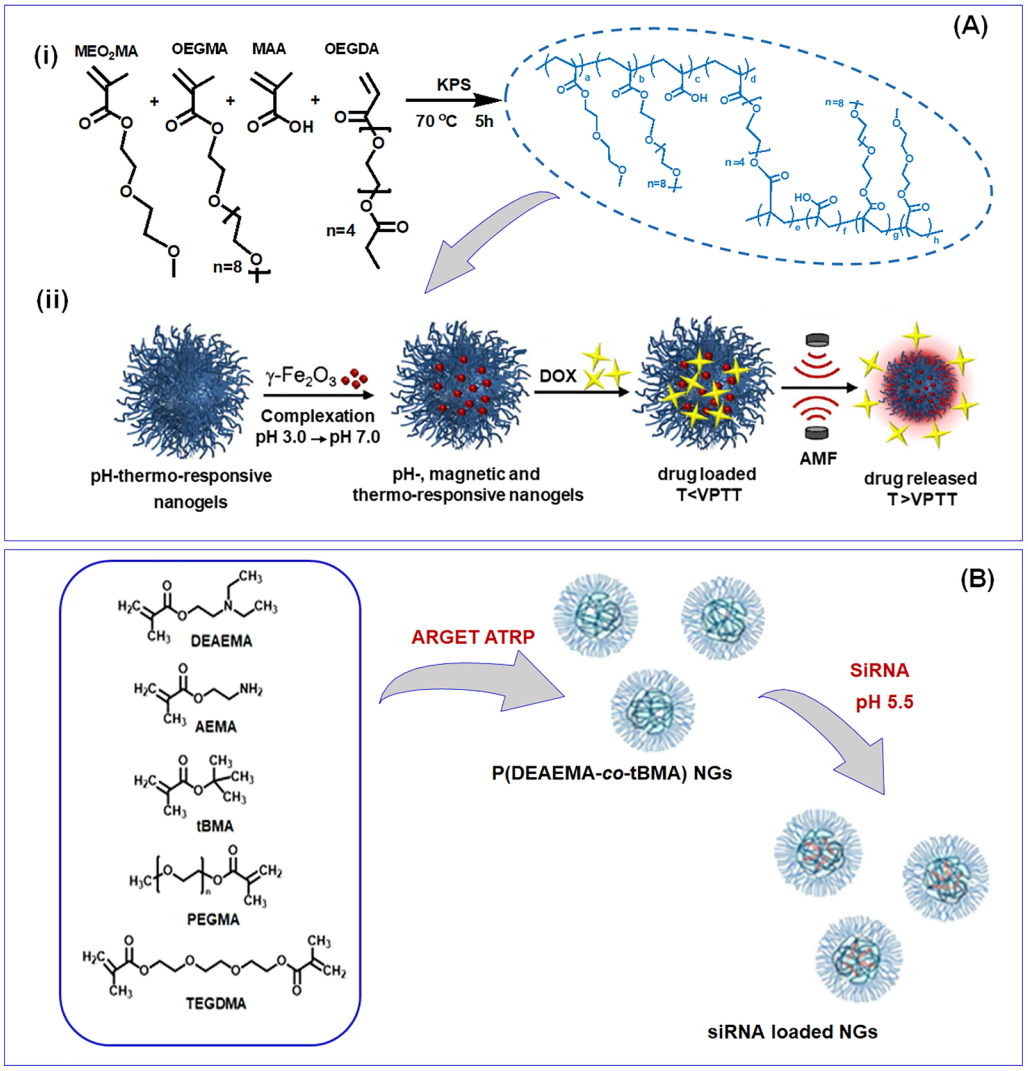

Figure 2. (A) (i) Illustration of magnetic nanogel synthesis through conventional aqueous precipitation radical copolymerization reaction of oligo(ethylene glycol) methacrylate monomers. (ii) The fabrication of a magnetic nanogel and loading and release of doxorubicin under an alternative magnetic field. Reprinted with permission from ref 14. Copyright 2017 American Chemical Society). (B) Synthesis of p(DEAEMA-*co*-tBMA) nanogels through ARGET ATRP and subsequent siRNA encapsulation. Reprinted with permission from ref 12. Copyright 2016 American Chemical Society.

has paramount importance for *in vivo* experiments, which can be extended by the stable chemical cross-links of the NGs. Besides, the hydrophilic, biodegradable NGs can endow the reversible responsive properties, and therefore, cross-linked NGs displayed tremendous potential for diverse theranostic applications compared to nanospheres, vesicles, micelles, dendrimers, etc.

Herein, we outline the developmental strategies of representative single, dual, multistimuli, and composite/hybrid "smart" NGs derived from various natural or synthetic polymers. Subsequently, the relevant and important applications of "smart NGs", the controlled release of drug and genetic materials, photodynamic therapy (PDT), photothermal therapy (PTT), bioimaging, and sensing were addressed. The important synthesis strategies, therapeutic release, cellular uptake characteristics, and *in vivo* results were highlighted. The current clinical scenario of NGs and the major challenges toward clinical translation of various NGs were also addressed.

2. SYNTHESIS STRATEGIES OF SMART NANOGELS

A variety of approaches are available to synthesize different stimuli-responsive NGs since the macromolecular engineering has witnessed a great advancement in the past decades. The NGs with required characteristics and pharmacologic effects can be synthesized for a specific therapeutic or diagnostic application by either a single strategy or combining different synthesis strategies. The current synthesis approaches can be generally categorized as follows: (i) the monomer polymerization in a heterogeneous or homogeneous environment; (ii) the self-assembly of appropriate polymers; (iii) the cross-linking of appropriate polymeric architectures; and (iv) template-assisted NG synthesis, etc. Among diverse polymerization techniques, the free radical polymerization[10] was the conventional approach in constructing NGs. However, in the past decades, several other "living" radical polymerization strategies like reversible addition−fragmentation chain transfer (RAFT),[11] atom transfer radical polymerization (ATRP),[12] *N*-carboxy-anhydride (NCA) ring-opening polymerization (ROP), etc.[13] have also emerged as versatile tools in the synthesis of "smart" NGs. To date, a wide

https://dx.doi.org/10.1021/acsomega.0c05276
ACS Omega 2021, 6, 5075−5090

range of polymers were used in the construction of "smart" NGs through conventional or advanced polymerization techniques combined with other macromolecular synthesis/fabrication strategies. In the subsequent sections, we discuss the diverse synthesis strategies of representative stimuli-responsive NG systems designed for various biomedical applications.

2.1. Free Radical Polymerization. Hajebi et al. have described the synthesis of temperature-responsive NGs with hollow cavities through precipitation-free radical polymerization of *N*-isopropylacrylamide (NIPAM) and vinyl-functionalized nanosilica. In a typical synthesis, the authors grafted 3-(trimethoxysilyl) propyl methacrylate (MPS) into silica nanoparticles after surface hydrolysis. Subsequently, the hollow poly(*N*-isopropylacrylamide) (PNIPAM) NGs were achieved by polymerizing NIPAM and MPS initiated by potassium persulfate (PPS) at 70 °C and cross-linking with *N*,*N*-methylene bis(acrylamide) (MBA) with various concentrations. The hybrid NGs were collected after centrifugation and hydrolyzed in an aqueous solution of hydrofluoric acid to remove the inorganic core and to obtain hollow NGs. These NGs demonstrated higher swelling/squeezing due to the hollow cavities, and the dynamic light scattering (DLS) investigation confirmed that hollow NGs are larger in size (above 300 nm), compared to hybrid NGs. Notably, NGs displayed smaller size at enhanced cross-linking structures, and NGs were found to be shrinking at elevated temperature conditions. Interestingly, the hollow cavities of the NGs were used as drug depots, as demonstrated by their higher doxorubicin (Dox) loading capacity due to the hollow cavities.[4]

The temperature and pH dual-triggerable copolymer poly(*N*-isopropylacrylamide-*co*-acrylic acid) (NIPAM-*co*-AA) was synthesized by Su et al. through free radical precipitation polymerization. Herein, NIPAM and MBA were dissolved in water. Calculated amounts of acrylic acid (AA) and surfactant sodium dodecyl sulfate (SDS) were added and subsequently polymerized at 70 °C by initiating with PPS, and the polymer was purified through dialysis. The authors also demonstrated further functionalization with bovine serum albumin (BSA) with fluorescent nature, and gold nanoclusters (AuNCs) were decorated in the NG surface. Besides, the NGs were further decorated with a tumor-targeting iRGD peptide, by coupling onto the BSA surface, and demonstrated spherical or flower-like morphology with around 150 nm in size and negative zeta potential values (−15 to −20 mV).[10]

A multistimulus (pH, temperature, and magnetic) responsive NG was developed by Cazares-Cortes et al. through precipitation radical copolymerization in a batch reactor. This NG preparation was achieved without the addition of any surfactants, and the NGs were composed of oligo(ethylene glycol) methacrylate (macro)-monomers (OEGMAs) and methacrylic acid (MAA). In a typical synthesis, di(ethylene glycol) methyl ether methacrylate (MEO_2MA), MAA, OEGMA, and cross-linker oligo(ethylene glycol) diacrylate (OEGDA) were polymerized in the presence of PPS initiator to obtain the NGs, and finally the NGs were purified by dialysis against distilled water (Figure 2A). Herein, the authors synthesized a NG with covalently linked rhodamine (RHB) for the intracellular tracking Dox release. Besides, superparamagnetic nanoparticles (γ-Fe_2O_3) encapsulated with NGs were also fabricated, and Dox was encapsulated (DLE of 63%) through a diffusion process. The final magnetic NGs have hydrodynamic diameter (R_H) between 328 and 460 nm and possess reversible swelling−shrinking characteristics at the volume phase temperature transition (VPTT) at 47 °C and in pH 7.5.[14] In another study, temperature/redox dual-responsive as well as zwitterionic NGs encapsulated with indocyanine green (ICG) and Dox were developed by Li and co-workers. The blank NGs were prepared through the precipitation free radical polymerization from a calculated amount of NIPAM, zwitterionic sulfobetaine methacrylate (SBMA), MAA, and *N*,*N*′-bis(acryloyl) cystamine (BAC) with SDS by triggering the polymerization by the addition of PPS at 75 °C. The ICG and Dox encapsulated NGs were subsequently fabricated, and the loading capability of the NGs was 4.5% and 4.75% for Dox and ICG, respectively. The DLS analysis revealed that the R_H was about 110 nm at physiological pH and 25 °C. The NG displayed spherical morphology and exhibited a temperature-dependent size reduction.[15]

Kim et al. reported diamond NG-implanted contact lenses which mediate the enzyme-dependent therapeutic delivery. In this work, the authors initially synthesized the N-acetylated chitosan, followed by the aerial oxidation of a lyophilized pristine nanodiamond (ND). The NDs solubilized in dimethyl sulfoxide (DMSO) under ultrasonication and NHS as well as EDC were added. Subsequently, reacting with polyethylenimine (PEI) obtained ND-PEI, and linking through succinic acid obtained carboxyl-functionalized ND-PEI. Finally, the cross-linking of chitosan (acetylated) and ND-PEI after NHS activation with drug timolol obtained the drug-loaded NG. The contact lenses were fabricated by copolymerizing the suspension of ND-NGs in 2-hydroxyethyl methacrylate (HEMA) and photopolymerizing after mixing of MAA, ethylene glycol dimethacrylate (EGDMA), and the photoinitiator.[16]

Chen et al. synthesized multistimuli (photo, pH, and redox) triggerable poly(acrylic acid-*co*-spiropyran methacrylate) (PAA-*co*-PSPMA) NGs. Typically, a photoresponsive methacryloyl monomer (SP-MA) was subjected to emulsion polymerization with pH-responsive AA, and SDS cross-linked through BAC resulted in NGs of 40−70 nm size, confirmed by DLS and transmission electron microscopy (TEM). The NGs swelled under ultraviolet (UV) light exposure due to isomerization of spiropyran to merocyanine (hydrophilic to hydrophobic) under acidic conditions, which enhances the hydrophilicity of the NGs, resulting in an increase in the size up to 250−350 nm. The drug loading was accomplished into the NGs for drug delivery and fluorescence cell imaging applications.[17] A light and photo-triggerable NGs were used for image-guided photothermal chemotherapy. A typical synthesis of the NG is based on PNIPAM and poly(*N*-isopropylmethacrylamide) (NIPMAM) in an equal ratio and cross-linking through acrylated dPG. The semi-interpenetration of thermoresponsive NGs was also achieved with polypyrrole (PPY). Notably, the semi-interpenetrated NGs displayed a size around 200 nm, with an enhanced encapsulation efficiency (20%) for the anticancer drug methotrexate (MTX) compared to NGs with no semi-interpenetration.[18]

A pH-responsive supramolecular NG was synthesized through metallo-supramolecular coordination of histidine, zinc (Zn-Por), and tetraphenylporphyrin (TPP) for synergistic chemo-PDT. In this work, initially they synthesized Zn-Por by reacting TPP with $Zn(Ac)_2{\cdot}2H_2O$. Simultaneously, histidine-modified dextran (DH) was synthesized from dextran and histidine through EDC coupling. The NG was then fabricated by reacting DH and Zn-Por in DMSO followed by dialysis (Figure 4A). The DLS experiments indicated that the size of NGs was 73 nm and underwent pH-responsive dissociation and reassocia-

https://dx.doi.org/10.1021/acsomega.0c05276
ACS Omega 2021, 6, 5075−5090

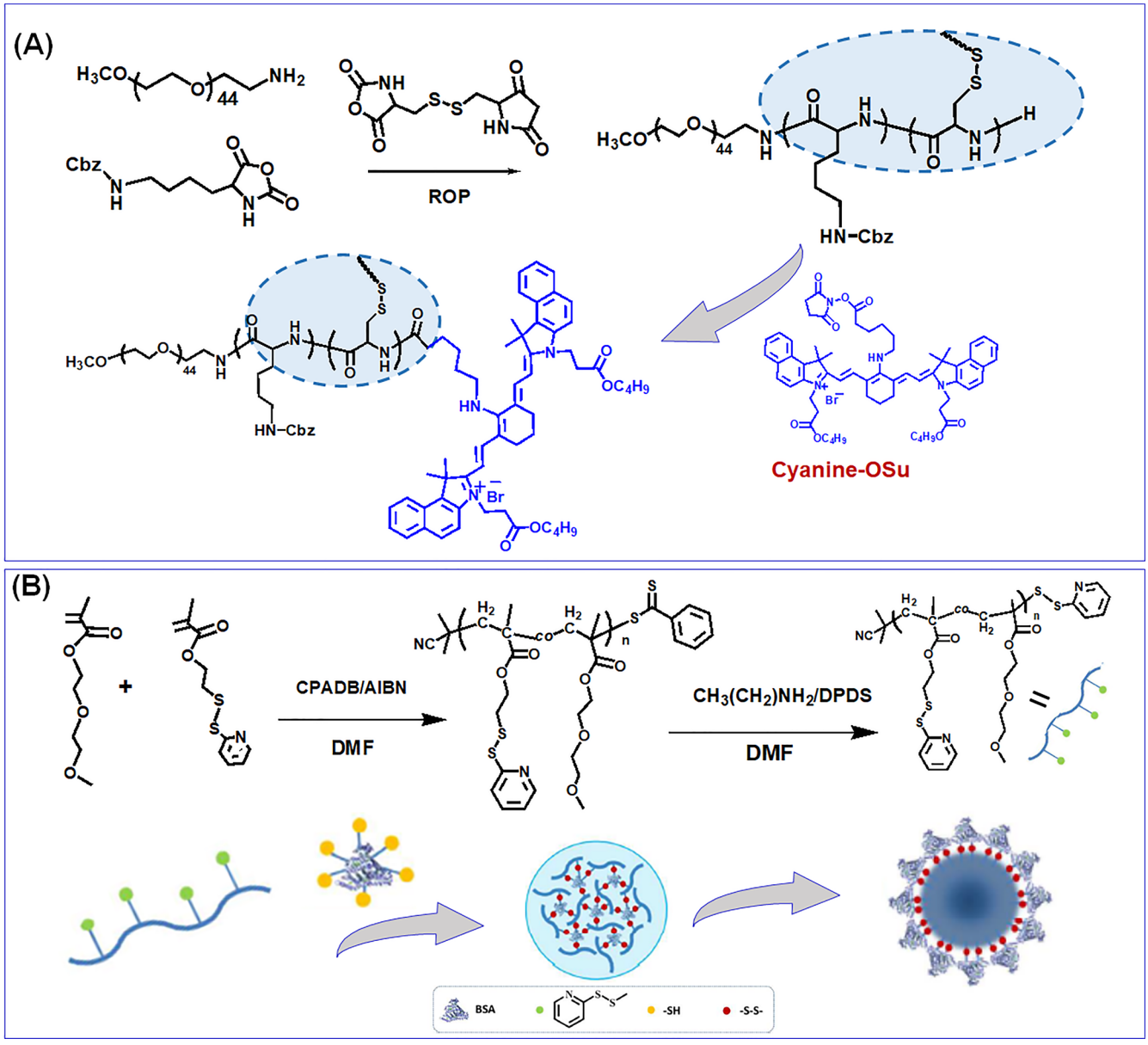

Figure 3. (A) Synthesis of near-infrared fluorescent and reduction-sensitive polypeptide nanogels through *N*-carboxy-anhydride (NCA) ring-opening polymerization of L-lysine and L-cystine NCA and subsequent conjugation of cyanine dyes. Reprinted with permission from ref 13. Copyright 2012 American Chemical Society. (B) The reversible addition−fragmentation chain transfer polymerization synthesis of random copolymers with pendant pyridyldisulfide groups and the fabrication of biohybrid nanogels demonstrate the structural transition above the lower critical solution temperature. Reprinted with permission from ref 25. Copyright 2016 American Chemical Society.

tion. The NG successfully entrapped Dox with significant DLC and DLE (5.32% and 36.7%).[19] Hang et al. developed light-degradable hyaluronic acid (HA) NGs for anticancer release applications. The light-responsive (infrared (NIR) and UV) NGs were fabricated from a graft polymer of HA and 7-*N*,*N*-diethylamino-4-hydroxymethylcoumarin (HA-CM). The NGs were fabricated by the dropwise addition of phosphate buffer to the HA-CM solution in methanamide/DMF followed by dialysis. The DLS results showed that the NGs possess negative surface charge and an R_H of 147 and 165 nm. However, the TEM data demonstrated 40−80 nm size, and the size discrepancies were attributed to the NG dehydration and shrinkage while drying. Dox was successfully encapsulated into NGs, without any notable size variation, and the DLE was 57−83%.[20] Li et al. reported biodegradable and glucose-responsive PNIPAM-based NGs composed of phenylboronic acid (PBA) as well as nitrilotriacetic acid (NTA) functionalities, cross-linked with EGDMA. Herein, the NTAs were introduced into the NG system to selectively bind insulin through zinc-ion-mediated chelation.[21]

2.2. RAFT Polymerization. Other than conventional polymerization techniques, the modern "living" radical polymerization strategies have also emerged as an excellent tool for nanogel fabrication. For instance, Ahmed et al. reported tailor-made pH and thermosensitive cationic glyco-NGs for small interfering ribonucleic acid (siRNA) delivery through the RAFT polymerization. In a typical synthesis, calculated amounts of poly(2-gluconamidoethyl methacrylamide) and 2-aminoethyl-methacrylamide were dissolved in deionized water, and subsequently, methoxydiethylene glycol methacrylate, the

https://dx.doi.org/10.1021/acsomega.0c05276
ACS Omega 2021, 6, 5075−5090

cross-linker, and the chain transfer agent (CTA) in 1,4-dioxane were added and polymerized at 70 °C. Subsequently, the epidermal growth factor receptor (EGFR)−siRNA was complexed with positively charged NGs. The glyco-NGs showed a size of 100−200 nm diameter, and the siRNA complexes maintained a net positive charge confirmed by DLS.[11] A cationic multistimuli-triggerable (pH, temperature, as well as enzyme) PAA-*b*-PNIPAM-protein NG was fabricated to deliver chemotherapeutic drug (Dox) and photosensitizer (Rose bengal). The copolymer PAA-*b*-PNIPAM was synthesized through RAFT from 2-(dodecyl sulfanyl thiocarbonyl sulfanyl)-2-methylpropionic acid as a CTA, initiated with 2,2′-azobis(isobutyronitrile). Subsequently, the PAA-*b*-PNIPAM NGs were fabricated by direct heating of PAA-*b*-PNIPAM aqueous solution above their lower critical solution temperature (LCST). Finally, protamine/PAA-*b*-PNIPAM NGs were synthesized through a polyelectrolyte complexation, and the charge interaction among PAA and protamine was established as a result of hydrogen bonding. Notably, the NG size and surface charge depended on the weight ratio of protamine and PAA-*b*-PNIPAM as well as pH.[22]

Massi et al. synthesized enzyme-temperature-responsive NGs with peptide cross-linking for the triggered delivery of biomolecules. Herein, a series of copolymers of PNIPAM, *N*-cyclopropylacrylamide (PNCPAM), and PNIPAM-*co*-NCPAM with various compositions were synthesized through RAFT polymerization. Subsequently, an inert hydrophilic block is the corona of the NGs, conjugated to a temperature-responsive block, which would achieve the self-assembly above the LCST. The PEG was used as a hydrophilic block, and either PNIPAM, PNCPAM, or its copolymer was used as a thermoresponsive block. A functional block composed of MAA and trimethylsilyl propargyl methacrylate was also incorporated to exert cross-linking with diazide-functionalized peptide after self-assembly and desilylation.[23] Farazi et al. have fabricated pH-labile MAA core cross-linked NGs through miniemulsion polymerization from the PEGMEMA−DMAEMA−*t*-BuMA terblock copolymer. Initially, the terblock copolymer was synthesized through RAFT polymerization, and subsequently the NGs were fabricated by the miniemulsion process of *t*-BuMA and cross-linked with EGDMA in water.[24] In another work, a virus-similar protein NG responsive to thermo-bioreduction dual stimuli was reported by cross-linking with temperature-responsive poly(di-(ethylene glycol) methyl ether methacrylate-*co*-2-(2-pyridyldisulfide) ethyl methacrylate) with reduced BSA through disulfide−thiol exchange chemistry for protein delivery (Figure 3B).[25] Chen et al. have reported an enzyme-, pH-, and GSH-responsive nanoaggregate composed of *N*-(1,3-dihydroxypropan-2-yl) methacrylamide (DHPMA) and PEG (pDHPMA-Dox-*SS*-mPEG) through RAFT polymerization. Herein, a peptide, GFLGKGLFG, was used to link the DHPMA-derived polymeric architectures. The Dox was conjugated to the polymer through a pH-labile hydrazone bond, and PEG was grafted onto the polymeric chain through a GSH-responsive *SS* bond. The R_h of the pDHPMA-Dox-*SS*-mPEG nanoaggregate displayed a size of 30 nm.[26] In another contribution, the same group developed branched poly(*N*-(2-hydroxy-propyl) methacrylamide)-based paclitaxel (PTX) conjugated nanoparticles (NPs) with dual-imaging agents Gd-DOTA and Cy5.5 (pHPMA-PTX-Gd-Cy5.5) through "one-pot" RAFT polymerization for image-guided antitumor therapy.[27]

2.3. NCA Ring-Opening Polymerization. A bioreduction-responsive *SS* cross-linked polypeptide NG with NIR fluorescence, for image-guided therapeutic delivery, was developed by Xing and co-workers. In this work, a dye was first obtained by reacting quaternary ammonium salt in the presence of bisaldehyde in a benzene−butanol solvent mixture. In the following, the dye was functionalized to aminocyanine by reacting with aminocaproic acid and further chemically modified to a succinimide function by reacting with *N*-hydroxysuccinimide in the presence of *N*-dicyclohexylcarbodiimide. Finally, the NGs was fabricated through ROP of carbobenzoxy-L-lysine and L-cystine NCAs initiated by aminoterminated PEG methyl ether in DMF and the NIRF NGs fabricated by the peptide coupling reaction (Figure 3A). The Dox was encapsulated into the NG to prepare the NIRF prodrug with a DLC and DLE of 11.2% and 70%, respectively. The mean diameter of the parent NG and NIRF NG was 275 and 232 nm, as observed from DLS measurement.[13] Ding et al. produced pH- and bioreduction-responsive NGs based on mPEG-p(L-lysine-*co*-L-cystine) through NCA ROP. Subsequently, the succinic, maleic, and aconityl derivatives of Dox were encapsulated, and the cellular accumulation and proliferation inhibition capabilities were investigated.[28]

2.4. Atom Transfer Radical Polymerization. To achieve oral administration of siRNA, Peppa's group developed enzyme-pH dual-responsive NGs for inflammatory bowel diseases (IBD) therapy. Herein, the polycationic p(DEAEMA-*co*-tBMA) NGs were synthesized using ATRP in emulsion (Figure 2B). After purification, the polymer was labeled with 4-chloro-7-nitrobenzofurazan, and the NG was loaded with a predesigned siRNA, able to target TNF-α. In the following, the microgel fabricated from p(MAA-*co*-NVP) was developed through photopolymerization. The peptide cross-linked gels were fabricated by reacting p(MAA-*co*-NVP) non-siRNA-loaded nanogels with GRRRGK peptide in an ethanol/water mixture through ethyl dicyclohexylcarbodiimide/*N*-hydroxysuccinimide (EDC/NHS) mediated coupling. Similarly, in another fabrication procedure, the NGs were first encapsulated with control and TNF-α siRNA and earlier loading in p(MAA-*co*-NVP) gel, and subsequently, the siRNA was allowed to undergo electrostatic complexation. From DLS analysis, a notable increase in R_h was observed in variation to the pH from 7.4 to 5.5 (∼110 to ∼122 nm) and also displayed a zeta potential (19 mV), found to be slightly decreased (17 mV) upon loading with negatively charged siRNA.[12]

2.5. Emulsion Techniques. Zou et al. synthesized a polyethylenimine-derived NG (PEI NG) through inverse miniemulsion polymerization, and Fe_3O_4 NPs were incorporated with Dox for image-guided chemotherapy. In atypical fabrication, citrate-stabilized Fe_3O_4 NPs were prepared, followed by the NGs being synthesized by reacting a calculated amount of *N*,*N*-methylene-bis(acrylamide) (BIS), Span 80, and PEI in a toluene−water solvent system followed by emulsification through sonication. In the following, triethylamine was added into solution to initiate the BIS cross-linking of PEI. The abundant amine surface of the PEI NGs was then modified with Fe_3O_4 NPs and finally neutralized the rest of the amine surfaces. The blank PEI NGs displayed an R_h of 180 nm; however, after covalent conjugation of Fe_3O_4 NPs (27 nm), the R_h of the NGs was increased to 251 nm, and the final acetylation led to a further increase to 264 nm. However, the initial surface potential was 38.9 mV, which decreased to 13.3 mV during the NG functionalization.[29]

By using an inverse miniemulsion technique, a temperature-redox-triggerable NG was constructed using poly(*N*-vinyl

https://dx.doi.org/10.1021/acsomega.0c05276
ACS Omega 2021, 6, 5075−5090

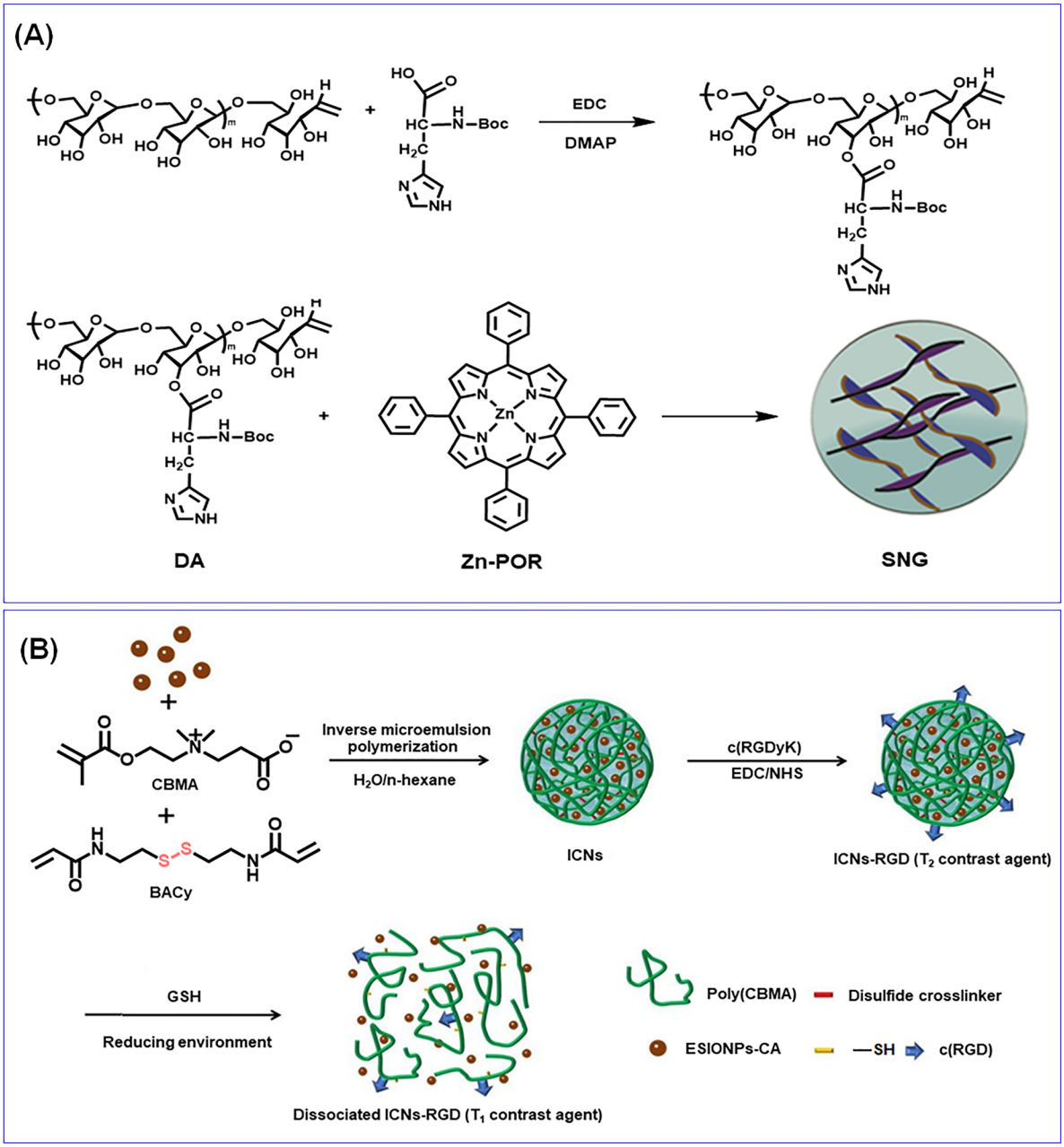

Figure 4. (A) Synthetic route for histidine-modified dextran and the fabrication of pH-responsive metallo-supramolecular nanogels. Reprinted with permission from ref 19. Copyright 2015 Elsevier. (B) Preparation of extremely small iron oxide nanoparticles encapsulated with poly(carboxybetaine methacrylate) nanogels and modification with the c(RGD) ligand as an activatable MRI contrast agent with switchable function from a T_2 contrast agent to a T_1 one through the stimuli-responsiveness toward glutathione. Reprinted with permission from ref 32. Copyright 2020 American Chemical Society.

caprolactam) (PNVCL) and Fe_3O_4. The Fe_3O_4 was initially subjected to surface modification with IEM. For emulsification, P(E/B)-PEO used as a surfactant and isopar M were used as an isoparaffinic hydrophobic solvent, and the mixture was then emulsified with polar dispersion containing NVCL, BAC, and $NABF_4$. Upon sonication, the miniemulsions were formed, and after adding azobis(isobutyronitrile), the mechanical stirring at 70 °C yielded temperature-redox-responsive PNVCL/Fe_3O_4 NGs.[30] A pH- and redox-responsive NG and its Dox-encapsulated NG were synthesized from oxidized dextran and PVA through a single emulsion technique. In a typical synthesis procedure, a calculated amount of oxidized dextran, Dox in PVA aqueous solution, and triethylamine were reacted to synthesis the prodrug. The cystamine dihydrochloride (CYS) was dissolved in PVA solution with triethylamine, and finally, the solutions were combined with chloroform separately, stirred to obtain the emulsion, and stirred for cross-linking. The chloroform was evaporated to obtain the final NG.[31] A bioreducible NG-based T1 contrast agent was used for magnetic resonance imaging (MRI) of a tumor created by Cao and co-workers. The Fe_3O_4 nanoparticles and citric-acid-modified ESIONPs (ESIONPs-CA) were initially synthesized. The SIONP-packaged poly(carboxybetaine methacrylate) NGs were fabricated by mixing a calculated amount of ESIONPs-CA in water and carboxybetaine methacrylate, and BAC and PPS were added to *n*-hexane with Tween 80 and Span 80

https://dx.doi.org/10.1021/acsomega.0c05276
ACS Omega 2021, 6, 5075−5090

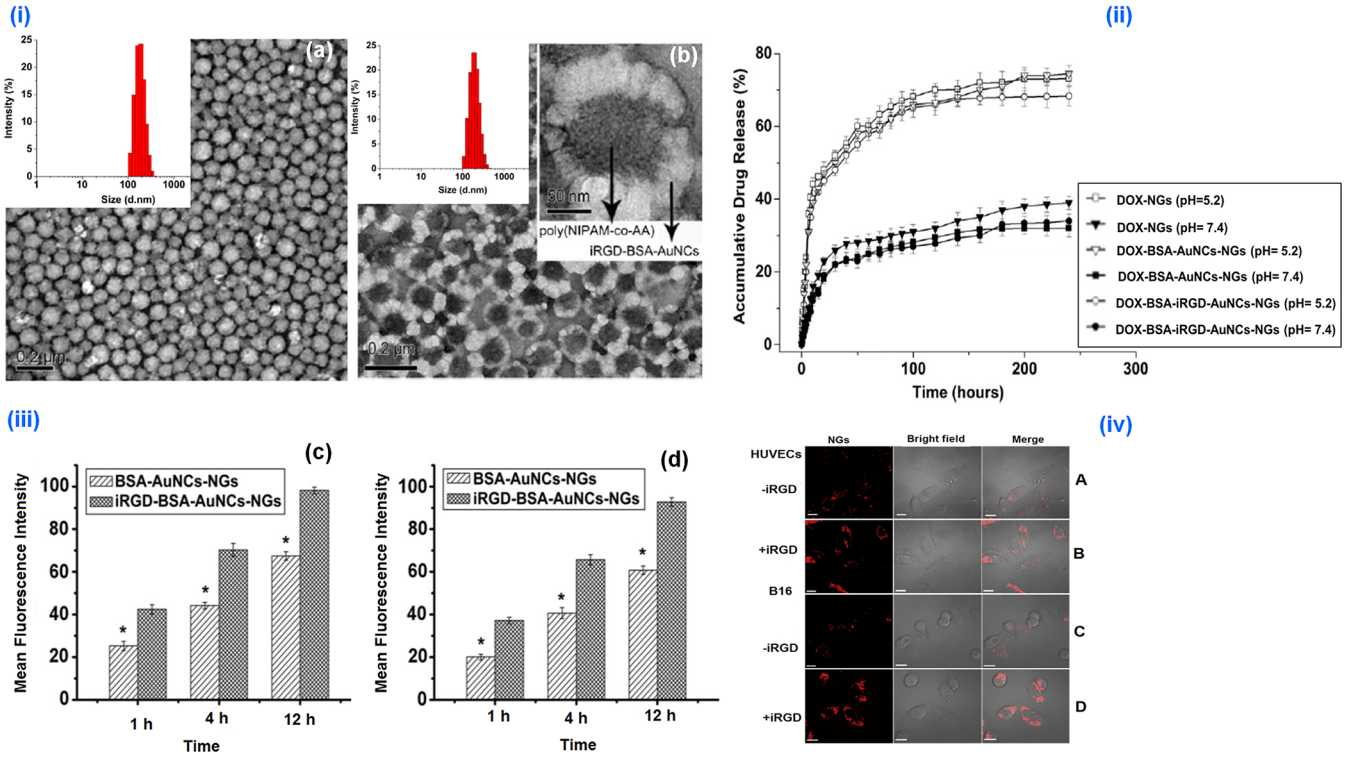

Figure 5. (i) TEM and DLS characterization of Dox-NGs (a) and Dox-iRGD-BSA-AuNCs-NGs (b). Dox-iRGD-BSA AuNCs NGs. (ii) The *in vitro* release profiles of Dox from various Dox-loaded NGs at 37 °C in PBS of different pH. (iii) The cellular uptake of different Dox formulations in HUVECs (c) and B16 (d) cells after 1, 4, and 12 h incubation. (iv) The intracellular delivery of BSA-AuNCs-NGs (A and C) and iRGD-BSA-AuNCs-NGs (B and D) in HUVECs (A and B) and B16 cells (C and D). The cells were incubated with BSA-AuNCs-NGs and iRGD-BSA AuNCs-NGs at 250 μg/mL for 4 h at 37 °C and then detected by confocal microscopy. Reprinted with permission from ref 10. Copyright 2013 Elsevier.

(Figure 4B). The mixture was mixed and sonicated to a stable microemulsion and heated to 65 °C, and the final NG (120 nm) was purified by washing with tetrahydrofuran and dialysis. The NGs were further modified with cRGD to achieve tumor targetability.[32] Li et al. have synthesized PNIPAM NGs with different cross-linking density and a series of poly(*N*-isopropylacrylamide-*co*-*N*,*N*-dimethylacrylamide) NGs (133−250 nm in size from DLS), with different monomer compositions developed through emulsion polymerization. The NGs were employed to prevent the crystallization hydrophobic drug, and the authors selected phenytoin as the model hydrophobic drug to assess the performance of NGs for drug solubility and dissolution efficacy. Herein, complete release of phenytoin was achieved in 6 h from PNIPAM NGs, and phenytoin was encapsulated through spray drying from solution into micron-sized amorphous powder particles.[33] In the following sections, we elaborate the representative therapeutic as well as diagnostic approaches with the above-mentioned smart NGs.

3. THERAPEUTIC AND DIAGNOSTIC APPLICATIONS OF SMART NANOGELS

3.1. Drug Delivery. Dox is one of the most common drugs used for chemotherapy of various malignancies. However, it was apparent that free Dox can induce several systemic side effects and can be reduced by loading the drug in NGs. Temperature−pH dual-responsive Dox-encapsulated (DLC-21.6% and DLE-90.2%) fluorescent NGs (iRGD-BSA-AuNCs-NGs) were successfully employed for controlled, targeted Dox delivery in extravascular tumor and endothelial cells. The *in vitro* Dox release under simulated physiological conditions (pH 7.4) and tumor acidic environment (pH 5.2) confirmed the feasibility of triggered as well as targeted release of Dox into B16 tumor cells. The blank NGs did not induce any cytotoxicity to the HUVECs and B16 cells. Even though free Dox and Dox-iRGD-BSA-AuNCs-NGs showed higher toxicity toward both cells after 24 and 48 h of incubation, Dox-iRGD-BSA-AuNCs-NGs showed an increased and delayed apoptosis (after 48 h) in both cell lines compared to free Dox due to iRGD functionalization. The confocal laser scanning microscopy (CLSM) visualization confirmed the significantly stronger fluorescent signal (Figure 5), in the cells treated with iRGD-BSA-AuNCs-NGs in contrast to other NG formulations.[10]

An NIR- and UV-light-triggerable HA-CM NG was employed for $CD44^+$-receptor-targeted delivery of Dox. The light exposure could initiate the destruction of the urethane linkage between CM and HA and cause superior release of internalized Dox. The Dox-loaded HA-CM NGs were treated with $CD44^+$ receptors and were overexpressed by MCF-7 cells, and the anticancer activity of drug-encapsulated NGs in the presence and absence of NIR exposure was confirmed through MTT assay U87 MG cells ($CD44^-$) as the control. The inherent fluorescence of Dox and coumarin, visualized in CLSM images, confirmed the NG internalization by the tumor through receptor-guided internalization, and the NIR exposure triggered intracellular Dox release.[20] A γ-Fe_2O_3-encapsulated pH, temperature, and magnetic-field-responsive oligo(ethylene glycol) methacrylate-based NG was constructed for Dox delivery. The drug release from the NG system was triggered by pH, temperature, and magnetic field (AMF). Notably, Dox diffusion was enhanced by increasing the temperature, decreasing the pH, and also applying the AMF. The magnetic field triggered cellular internalization of

https://dx.doi.org/10.1021/acsomega.0c05276
ACS Omega 2021, 6, 5075−5090

magnetic NGs and Dox-containing magnetic NGs, and free Dox was investigated in PC-3 cancer cells. The study confirmed that magnetic NGs demonstrated pronounced Dox release toward tumors with higher cytotoxicity compared to other formulations.[14]

NIPAM-based, temperature-responsive, hybrid-hollow NG structures were investigated for Dox loading and release. The delivery kinetics of Dox-encapsulated NGs was investigated at diverse temperature conditions. The Dox delivery was significant at temperatures below the NG disassembly temperature. Notably, the hollow NGs demonstrated an enhanced DLC. The higher cumulative release was observed for hybrid NGs, also confirmed by the Korsmeyer−Peppas models. The cytotoxicity Dox-loaded hollow NGs were evaluated in the HeLa cell line, which displayed higher toxicity, as a result of the release of a significant amount of Dox.[4] An enzyme-, pH-, and GSH-responsive Dox-conjugated (pDHPMA-Dox-*SS*-mPEG) nanoaggregate was developed for anticancer therapy. Herein, controlled release of Dox was observed as a result of the acidic pH and reductive microenvironment. Notably, around 87% of Dox was released from nanoassemblies with cathepsin B and GSH at pH 5.4. The cellular internalization mechanism of the pDHPMA-Dox-*SS*-mPEG nanoaggregates was evaluated in 4T1 cells. The results revealed that the nanoassemblies internalized into 4T1 cells through multiple endocytosis pathways, and Dox was released in the presence of acidic pH and reductive enzymes, which led to efficient apoptosis. The *in vivo* antitumor efficiency was examined using BALB/c mice bearing 4T1 tumors. Notably, the pDHPMA-Dox-*SS*-mPEG nanoassemblies showed better antitumor effect than free Dox at an equivalent dose and upon comparing other controls.[26]

In another contribution, magnetic-, temperature-, as well as redox-responsive PNVCL/Fe_3O_4 NGs were studied for the controlled 5-fluorouracil (5-FU) delivery. The NGs encapsulated higher drug loading capacity (400 mg g^{-1}), and sustained delivery of 5-FU was triggered by increasing the external temperature or under redox environments. The PNVCL/Fe_3O_4 NG biocompatibility was assessed toward SW620 cells and displayed lower toxicity.[30] A pH-redox dual-responsive oxidized dextran and PVA-derived NG were reported for Dox release to triple negative breast cancer cell lines. Herein, a high DLE was observed due to the conjugation of Dox through a pH-sensitive linkage. The dual sensitive NGs displayed an enhanced release of Dox under tumor pH and also under high GSH concentrations. The NG showed prolonged Dox release in MDA-MB-231 and in the mouse model.[31]

The chemical modification of Dox was also investigated as a significant strategy for developing prodrugs, to overcome the side effects. In this regard, pH- and reduction-responsive PEG-polypeptide NGs were fabricated, and the succinic, maleic, and acontityl derivatives of Dox were successfully encapsulated with ∼90 wt % of DLE which was several folds higher than free Dox. The *in vitro* drug release was pH and bioreduction dependent, and the cell internalization and growth inhibition activities of derivatized Dox were confirmed against HeLa and HepG2 cells.[28] To demonstrate protein delivery, BSA-encapsulated temperature-redox dual-responsive polymer−protein biohybrid NGs were reported, and the NGs undergo a structural change according to temperature variation. Below the LCST of the NG, model protein BSAs were encapsulated. Above the LCST, the disassembly of polymer chains results in the cores, and BSA moves to the NG shell. The cytotoxicity of NGs investigated toward MCF-7, 3T3, and 293T cells demonstrated negligible toxicity. The protein NGs were able to dissociate in the glutathione (GSH) environment, and BSA delivery occuring by destruction of the *SS* bonds was confirmed with SDS-PAGE.[25] Temperature and enzyme dual-responsive NGs were fabricated for enzyme-triggered protein delivery. Herein, the NG was responsive to matrix metalloproteinases (MMPs), overexpressed in inflammatory and cancer diseases. The encapsulation and delivery performance of enzyme-responsive NGs was verified with fluorescently labeled BSA. The excellent cell viability of the NGs was confirmed in RAW 264.7 cells, and the MMP-7-triggered NG disassembly and subsequent protein release kinetics were followed with fluorescence correlation spectroscopy.[23] Farazi et al. synthesized a pH-responsive NG system for efficient loading and intracellular release of charged hydrophilic peptides. The MAA core cross-linked NGs showed high loading capacity, by simple absorption from a pH 7.4 solution. Notably, at acidic pH, the peptide is quickly released from the NG due to the core collapse and inner shell protonation. A dye-labeled NG was fabricated to achieve Förster resonance energy transfer (FRET) capabilities to investigate NG performance in entrapment and rapid delivery of peptides, and cellular uptake was assessed with MCF-7 cell lines.[24]

Drug-incorporated contact lenses are an ideal treatment strategy for ophthalmic conditions such as glaucoma. Through a lysozyme-triggered release of an antiglaucoma therapeutic agent timolol maleate (TM), a diamond NG-embedded contact lens was constructed by Kim and co-workers. The contact lens device was able to mediate the controlled drug release from the NG through lysozyme-triggered polymer decomposition, which eliminates the uncontrolled release possibility. The released TM from the ND−NG lens retaining drug efficiency was assessed in trabecular meshwork cells.[16] Bifunctional NIPAM NGs composed of NTA and PBA were developed for the glucose-responsive release of insulin. The NTA groups were able to specifically bind imidazole-containing insulin by zinc-ion-mediated chelation, resulting in 66% of insulin loading capacity. Herein, the on−off controlled insulin diffusion was observed, and an enhanced release was due to the charge interactions and phase transition after glucose binding. MTT assay on mouse fibroblast cells (NIH 3T3) and the enzymatic degradation revealed excellent biocompatibility and degradability for the nanogels.[21] As an alternative strategy for dermal drug delivery, Gao et al. synthesized a supramolecular polymer NG through noncovalent molecular interactions. In this work, a supramolecular polymer NG loaded with dexamethasone (DEX) was fabricated by host−guest interactions, and interactions between the group pillar[5]arene and alkyl chains on the hyperbranched polyglycerol backbone were used for the cross-linking. The skin penetration characteristics of the NG were evaluated by comparing the individual host−guest polymer aggregates. The NGs demonstrated better DEX loading capacity and enhanced skin penetration compared to the individual host−guest polymer. The biocompatibility of the NG was verified by an MTT assay toward HaCat cells and displayed good viability after 24 h under specific NG concentrations. Besides, the *in vitro* skin permeation studies revealed that NGs improved the Nile red penetration through skin by multiple fold compared to the conventional therapeutics on a barrier-deficient skin model.[34]

3.2. Gene Delivery. The gene interference technology, which involves gene silencing, was studied for the treatment of diseases of genetic origin. The nanoassemblies like stimuli-responsive NGs for siRNA transport were an established

https://dx.doi.org/10.1021/acsomega.0c05276
ACS Omega 2021, 6, 5075−5090

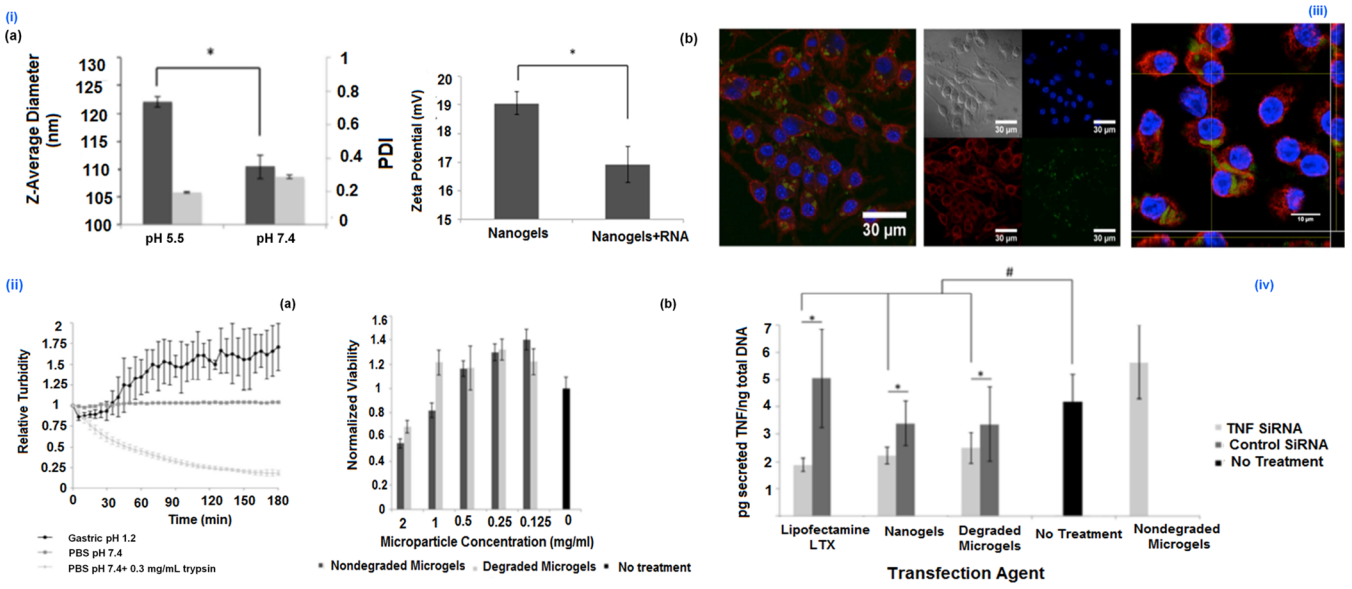

Figure 6. (i) (a) Hydrodynamic diameter of p(DEAEMA-*co*-tBMA) nanogels and (b) zeta potential measurements indicate a positive surface charge of ∼19 mV, which decreases slightly after loading with negatively charged RNA. (ii) (a) Relative turbidity measurements indicate that the microgel platform degrades in the presence of trypsin but remains intact in the presence of PBS or gastric fluid. (b) Relative viability of RAW 264.7 cells incubated with varying concentrations of degraded or nondegraded microgels for 24 h. (iii) (a) Bright-field/fluorescent panels and (b) Z-stack orthogonal images of RAW 264.7 macrophages incubated with degraded microgels containing P(DEAEMA-*co*-tBMA) nanogels. The released nanogels were efficiently uptaken by the RAW 264.7 cells (blue, DAPI; red, wheat germ agglutinin (membrane); green, NBD-Cl conjugated nanogels). (iv) TNF-α knockdown induced by siRNA carried by Lipofectamine LTX, p(DEAEMA-*co*-tBMA) nanogels, or degraded microgels containing p(DEAEMA-*co*-tBMA) nanogels. Reprinted with permission from ref 12. Copyright 2016 American Chemical Society.

approach by fabricating stable polyplexes that demonstrated enhanced knockdown properties. In this regard, the Narain research group developed positively charged glyco-nanogels for EGFR-targeted siRNA delivery to EGFRs in overexpressed ovarian carcinoma. Herein, the nanogel−siRNA complexes were formulated without serum proteins, resulting in higher siRNA entrapment, and cationic glyconanogel siRNA produced stable polyplexes of 400−500 nm in size. The cellular internalization of FITC-labeled siRNA NGs was confirmed in HeLa with/without serum proteins by using untreated HeLa cells as a negative control and showed an uptake ability around 30−40%. Notably, HeLa cell internalization of the NG−siRNA polyplex was found to be increased (60−80%) with serum protein. The EGFR-targeting siRNA nanocomplex treated HeLa cells investigated through in-cell ELISA for the confirmation of receptors.[11]

Enzyme−pH dual-active NGs were designed toward oral administration of siRNA, to target TNF-α. The siRNA delivery vehicle is a microgel, derived from P(MAA-*co*-NVP) which is cross-linked through an enzyme-sensitive peptide linkage. The polycationic NGs were loaded in enzyme-cleavable gels with a siRNA loading efficiency of greater than 90%. These NGs have demonstrated the efficient endocytosis of the siRNA and successful delivery to the cytosol. The internalization of NGs delivered was evaluated in RAW 264.7 cells and visualized using CLSM. Importantly, TNF-α siRNA-encapsulated NGs were delivered since enzyme-active microgels prompted TNF-α knockdown macrophages, demonstrating the capability of the therapeutic formulation (Figure 6).[12]

3.3. Photodynamic and Photothermal Therapy. The PTT with NIR light is an invasive paradigm, which can accomplish effective hyperthermia through penetration toward deep tissues by exposing to light-absorbing materials, like cyanine dyes as well as other photothermal nanosystems. In this regard, Li and co-workers developed a zwitterionic-, temperature-, and redox-sensitive NGs composed of NIR dyes ICG and Dox, which exhibited enhanced photothermal effects. Herein, the Dox release rate and HepG2 cellular uptake were found to be enhanced by the dual treatment with GSH and NIR irradiation. The *in vivo* activity was studied on H22-bearing mice models with various formulations followed by laser exposure. The drug release was on demand, triggered by the higher intracellular concentration of GSH and NIR-induced photothermal activity.[15] In another work, light- and temperature-responsive NIPAM-based semi-interpenetrated PPY NGs with similar VPTT as with noninterpenetrated formulations demonstrated good photothermal transducer photostability for photoacoustic contrast enhancement applications. Herein, the unique characteristics of PPY impart dual responsiveness. Herein, the encapsulation and release performance of MTX were evaluated, and enhanced release profiles were observed on exposing NIR light. The *in vitro* cytotoxic effects of the NG were studied on A549 lung carcinoma cell lines, and the A549 xenograft tumor-bearing mice model was employed to validate imaging-guided photothermal chemotherapy (Figure 7) of the NG, confirming the photothermal ablation of the tumor.[18]

Yao et al. synthesized a pH-labile supramolecular NG for simultaneous chemo PDT. Notably, metalloporphyrins were used as a photosensitizer in clinical PDT, due to the ease of generating toxic singlet oxygen. Herein, the Zn-Por was used to coordinate with histidine to develop a pH-responsive NG which was active in an acidic cancer environment for the triggered delivery of Dox and Zn-Por to induce tumor cell apoptosis. The nontoxicity and photodynamic toxicity of free NGs were confirmed on HepG2 and HeLa cells after incubating the NG under a different duration with and without light irradiation. The CLSM confirmed efficient cellular uptake of the NG by HepG2 cells. Besides, the *in vivo* antitumor effect of Dox-NG was studied in a B16F10 melanoma model. The Zn-Por of the NG possesses

https://dx.doi.org/10.1021/acsomega.0c05276
ACS Omega 2021, 6, 5075−5090

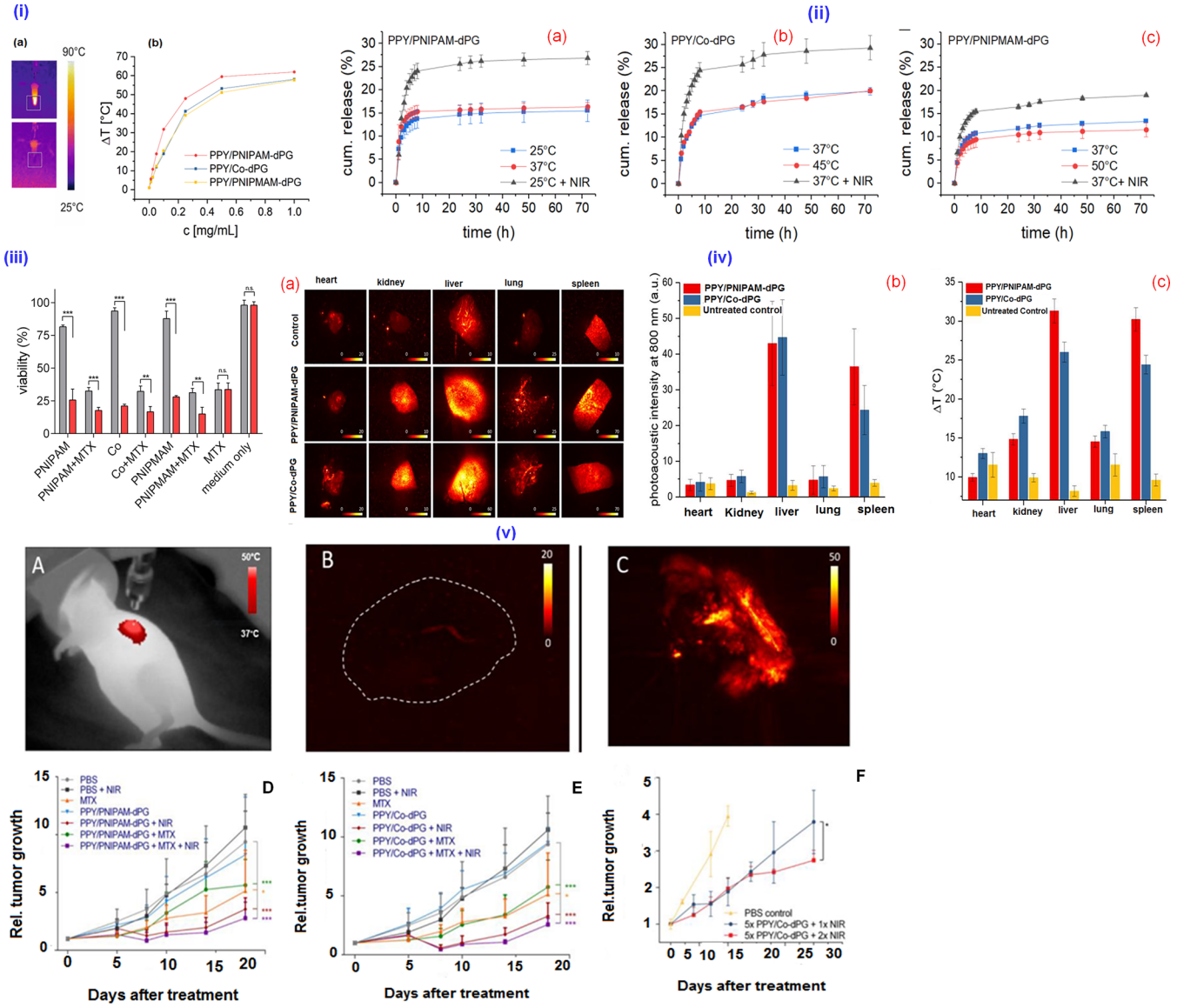

Figure 7. (i) Photothermal activity and thermoresponsiveness of the semi-interpenetrated PPY nanogels. (a) IR pictures of a sample during irradiation and (b) concentration-dependent temperature difference reached after 5 min of NIR irradiation. (ii) Release profiles of MTX above and below VPTT of semi-interpenetrated PPY nanogels upon NIR irradiation. (iii) Photothermal and combinational therapy in vitro. Cell viability of A549 lung carcinoma cell line determined by an MTT assay incubated for 48 h with MTX-loaded (10 wt %) and -unloaded PPY nanogels with and without exposure to NIR laser (785 nm, 500 mW) for 7 min. (iv) (a) $x-y$ MIPs of PA images of excised organs at 800 nm. (b) Mean PA image intensity of excised, formalin-fixed organs of a female nude mouse treated over five consecutive days with 100 mg/kg of PPY nanogels. (c) Photothermal response (max. ΔT after 5 min) of the same samples after irradiation with the output of a NIR lamp. (v) (A) IR image of mice under NIR irradiation with i.t. injected nanogels. (B) MIP of photoacoustic image (PI) of an untreated control. (C) MIP of PI of a tumor after injection of nanogels and 5 min NIR irradiation *ex vivo*. (D, E) Rel. tumor growth over time of mice treated i.t. with MTX-loaded various nanogels with and without exposure to NIR. (F) Rel. tumor growth over time after i.v. administration of five consecutive doses of PPY/Co-dPG and exposure to NIR (5 min) 48 h after the last injection with respect to controls. Reprinted with permission from ref 18. Copyright 2019 Elsevier.

the photosensitivity and generates an active oxygen species to achieve the combinatorial chemical as well as PDT.[19] In another notable study, multistimuli-responsive protamine/PAA-*b*-PNIPAM NGs were investigated for Dox and photosensitizer release against drug-resistant breast carcinoma. The NGs were efficiently loaded with rose bengal and Dox with a DLE of 54.9 and 52.3%, respectively, which caused significant damage toward breast carcinoma upon photoirradiation. The NG demonstrated pH-responsive Dox release, besides the release also sensitive to trypsin. The Dox and rose bengal loaded NGs demonstrated an improved MCF-7/ADR tumor inhibition efficiency because of chemo-photodynamic therapeutic effects.[22] Zhang et al. developed a glycodendron/pheophorbide-a (PPa)-decorated HA for cancer photodynamic therapy. In a typical synthesis, initially HA-conjugate polymers (HA-SS-Py and HA-SH) were synthesized, and subsequently HA-PPa-Dendron and HA-PPa were achieved through thiol−disulfide and thiol−maleimide reactions. The DLS analysis demonstrated an R_h of about 84 ± 6 nm for HA-PPa and 88 ± 612 nm HA-PPa-Dendron with zeta potential of −26 to −28 mV, respectively, in aqueous media. Herein, the HA-PPa-Dendron showed an increased apoptosis toward MBA-MB-231 cells *in vitro* and an enhanced PDT efficacy *in vivo* and confirmed the complete eradication of tumors in a MDA-MB-231 tumor-bearing BALB/

https://dx.doi.org/10.1021/acsomega.0c05276
ACS Omega 2021, 6, 5075−5090

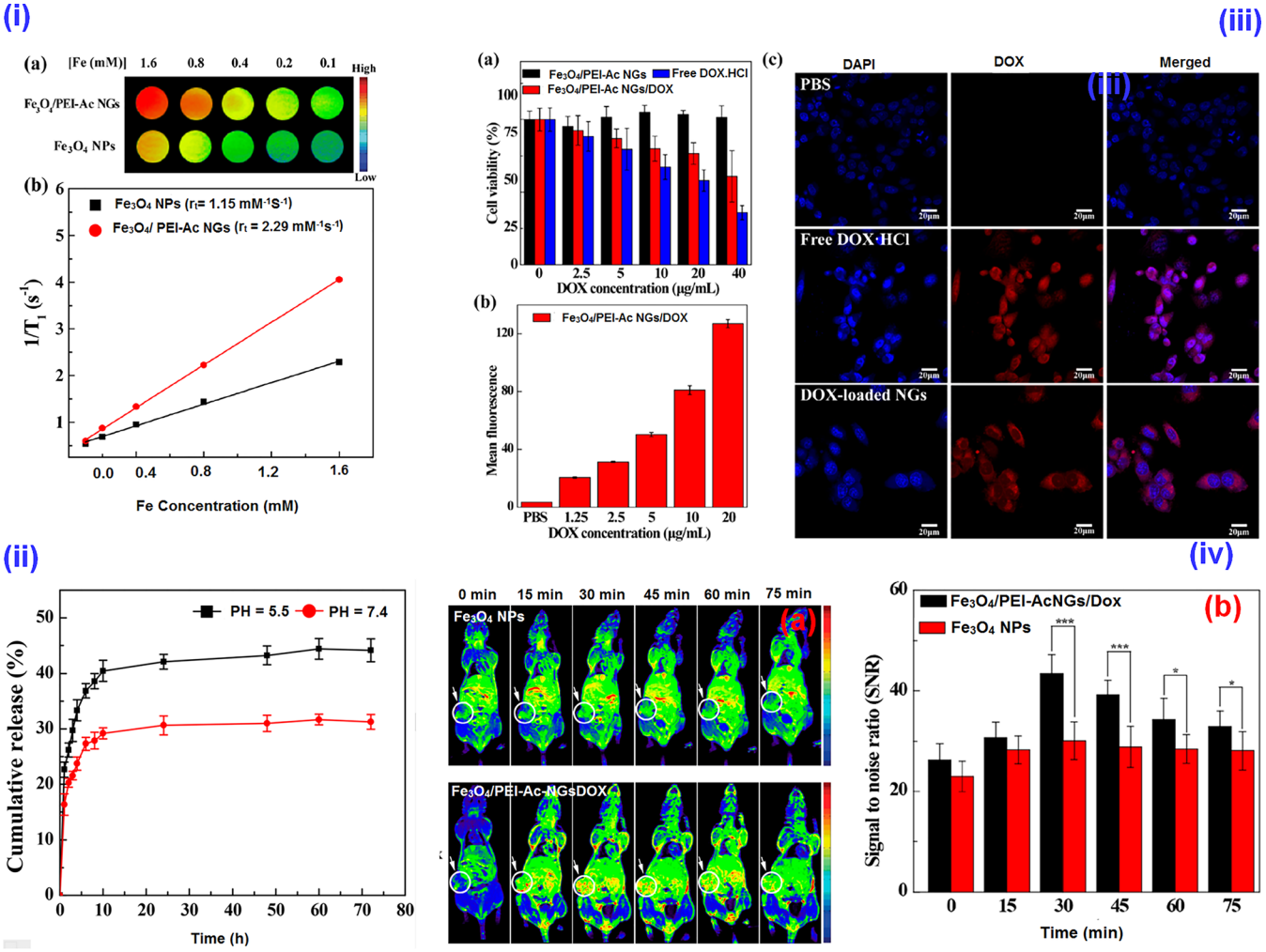

Figure 8. (i) (a) Color T_1-weighted MR images of the ultrasmall Fe_3O_4 NPs and Fe_3O_4/PEI-Ac NGs at different Fe concentrations, indicating the gradual increase of MR signal intensity. (b) Linear fitting of $1/T_1$ as a function of Fe concentration for the two different materials. (ii) The Dox release from the Fe_3O_4/PEI-Ac NG/Dox under different pH. (iii) (a) The CCK-8 assay of 4T1 cell viability after treatment formulations with different Dox concentrations for 24 h. (b) The mean fluorescence of cells treated with Fe_3O_4/PEI-Ac NGs/Dox as a function of Dox concentration. (c) Confocal microscopic images of 4T1 cells after treatment for 4 h with various formulations at 10 μg/mL of Dox concentration. (iv) The *in vivo* T_1-weighted MR images (a) and MR signal-to-noise ratio (b) of the xenografted 4T1 tumors before and at different time points post i.v. injection of Fe_3O_4 NPs or Fe_3O_4/NGs-Ac NGs/Dox (Fe mass = 150 μg, in 0.2 mL of PBS for each mouse). Reprinted with permission from ref 29. Copyright 2020, American Chemical Society.

c nude mice model under laser irradiation. The therapeutic effect was significantly higher for HA-PPa-Dendron than free PPa and HA-PPa.[35]

3.4. Bioimaging and Sensing. An image-guided drug release system provides the possibility of tracking the precise location of the drug delivery vehicles and provides beneficial data for both disease diagnosis and its successive therapy. For instance, Xing et al. demonstrated the successful bioreduction-responsive Dox delivery by using polypeptide NGs with NIRF characteristics. The *in vitro* Dox diffusion from NIRF NGs confirmed an enhanced release kinetics triggered by GSH. The viability assay in HeLa cells demonstrated that the NIRF NG was less toxic at higher concentration; however, the NIRF prodrug showed a higher toxicity at lower concentration due to the toxic effect of Dox. The successful endocytosis of the NIRF NG and NIRF prodrug was confirmed in A549 cells, and tumor localization capability was investigated through nude mice full body imaging. The *in vivo* experiments revealed that both formulations were localized in tumor tissues, and importantly, as a result of NIRF labeling, imaging of Dox delivery was achieved.[13] Chen et al. constructed a multistimulus (light, pH, and redox) active PAA-*co*-PSPMA NG for anticancer Dox delivery and fluorescence cell imaging. The NG displayed multiple stimuli-responsive Dox delivery profiles, due to spiropyranmerocyanine-isomerization-induced swelling of NGs under UV light and acidic pH. Similarly, in a reductive environment, the NGs were disassembled due to the destruction of an *SS* cross-linker. The cytotoxicity of NGs was assessed on MCF-7 cancer cells, before and after UV exposure, and Dox induced an enhanced and effective cancer cell apoptosis, after UV irradiation of NGs. Notably, the merocyanine moieties of NGs emit green fluorescence after internalization by MCF-7 cancer cells, which allows fluorescence cell imaging.[17]

A PEI-based hybrid NG composed of ultrasmall Fe_3O_4 NPs and Dox was developed for T1-weighted MRI and cancer therapy. The Dox-free NGs confirmed an excellent cytocompatibility toward 4T1 cells, and the hybrid NGs demonstrated pH-dependent Dox release. The therapeutic activity of the NGs was

https://dx.doi.org/10.1021/acsomega.0c05276
ACS Omega 2021, 6, 5075−5090

Table 1. Representative "Smart" Biocompatible Nanogel Systems and Their Synthesis Routes, Types of Experiments, Various Therapeutics, and Potential Therapeutic and Diagonostic Applications

nanogel system	synthesis method	therapeutics/ theranostic agent	type of experiment (*in vitro*/*in vivo*)	application	ref
PNIPAM NGs	precipitation-free radical polymerization	Dox	*in vitro* (HeLa cells)	drug delivery	4
P(NIPAM-*co*-AA) NGs	free radical precipitation polymerization	Dox	*in vitro* (HUVECs and B16 cells)	drug delivery	10
(PAA-*co*-PSPMA) NGs	emulsion radical polymerization	Dox	*in vitro* (MCF-7 cells)	drug delivery and cell imaging	17
P(NIPAM- PPY) NGs	free radical polymerization	MTX	*in vitro* (A549 cells) *in vivo* (A549 xenograft tumor bearing mice model)	photothermal chemotherapy	18
PNIPAM-*co*-NCPAM NGs	RAFT polymerization	protein	*in vitro* (RAW 264.7 cells)	protein delivery	23
cationic glyco-NGs	RAFT polymerization	siRNA	*in vitro* (HeLa cells)	gene delivery	11
p(DEAEMA-*co*-tBMA) NGs	ATRP	siRNA	*in vitro* (RAW 264.7 cells)	gene delivery	12
PEI NGs	miniemulsion polymerization	Fe_3O_4 NPs/Dox	*in vitro* (4T1 cells) *in vivo* (xenografted 4T1 breast tumor model)	MR image-guided chemotherapy	29
zwitterionic NGs	precipitation-free radical polymerization	indocyanine green (ICG)/Dox	*in vitro* (HepG2 cells) *in vivo* (H22-bearing mice)	photothermal therapy	15
PNVCL/Fe_3O_4 NGs	miniemulsion polymerization	5-fluorouracil	*in vitro* (SW620 cells)	magnetic guiding drug delivery	30
dextran NGs	emulsion polymerization	Dox	*in vitro* (MDA-MB-231 cells) *in vivo* (MDA-MB-231 cells mice)	drug delivery	31
poly(carboxybetaine methacrylate) NGs	emulsion polymerization	ESIONPs	*in vitro* (U87-MG cells) *in vivo* (tumor-bearing mice)	MR imaging	32
Ag@p[(VPBA-DMAEA)] NGs	free radical polymerization	insulin	*in vitro* (Cos7 cells)	glucose-sensing and insulin delivery	35
polypeptide NGs	NCA ring-opening polymerization	Dox	*in vitro* (A549 cells) *in vivo* (tumor-bearing nude mice)	image-guided drug delivery	13
supramolecular NGs	free radical polymerization	Dox/Zn-Por	*in vitro* (HepG2 and HeLa cells) *in vivo* (B16F10-heterografted melanoma model)	chemo-photodynamic therapy	19

assessed, and *in vivo* studies with hybrid NGs confirmed excellent MR imaging capabilities compared to free NPs. The chemotherapeutic efficacy of the NG was evaluated on the 4T1 tumor model by monitoring the tumor volume change, and the hybrid NG-treated mice maintained a survival rate of 80% without notable damages to other major organs. Conclusively, the hybrid NG was able to inhibit proliferation under a T1-weighted MRI (Figure 8).[29] In another work, a bioreducible NG-based T1 contrast agent for the MRI of tumors was developed. The ESIONP-based MRI can stimulate the GSH of tumor tissues to undergo switching from T2 to T1 contrast material. Herein, the RGD-functionalized NG exhibited excellent targetability. The bioreduction responsiveness of the NG examined on U87-MG cells and *in vivo* MRI of a tumor-induced animal model were studied and confirmed the targeting function as well as GSH-triggered MRI signal alteration. Conclusively, the contrasting capability of the tumor directed the NG toward an accurate tumor analysis.[32]

Gordon et al. studied the biodistribution of redox-responsive NIR-NGs by using fluorescence molecular tomography (FMT) of MDAMB-231-luc-D3H2LN mammary carcinoma. Herein, the authors formulated NGs of various sizes (28−135 nm), of PEG corona with various chain lengths with 50% PEG functionalization. The NGs were fabricated through self-assembly of random copolymers into the disulfide group for encapsulation and controlled release of cyanine dye Cy 7. The NGs were injected in a mice model with MDAMB-231-luc-D3H2LN carcinoma, and the *in vivo* biodistribution was assessed using FMT at various time durations postinjection and confirmed the tumor localization and retention over 72 h.[36]

Biomolecule-responsive NGs were also investigated for biosensing applications. For instance, a glucose-sensitive hybrid NG comprised of Ag NPs coated with a boronate derivative (Ag@p(VPBA-DMAEA)) was reported. The incorporation of a glucose-activable shell onto silver NPs makes polymer-decorated NPs responsive to glucose. The nanosilver imparts optical fluorescence, and polymer shells adopted the surrounding environment of glucose gradients and transformed the disruptions of the glucose level into optical indicators, which regulate the encapsulated insulin delivery. The NG cell viability was confirmed in Cos7 cells in a wide range of concentrations.[37] A multifunctional branched pHPMA-PTX-Gd-Cy5.5 NP consists of cyanine5.5 and Gd-DOTA as imaging agents, and PTX as a chemotherapeutic agent was developed by Cai and co-workers. The NPs demonstrated biocompatibility and high stability under physiological conditions, whereas in the tumor milieu, the NPs demonstrated stimuli-responsive disassembly and the subsequent release of PTX. The *in vitro* investigation of fluorescent-dye-labeled NPs displayed high toxicity toward 4T1 carcinoma. Notably, the presence of cathepsin B in the tumor microenvironment is capable of degrading the polymer backbone and the selective release of PTX to tumor cells. Besides, the anticancer efficacy was tested with the 4T1 xenograft mouse model and confirmed the reduction of the tumor volume, which was detected by MRI compared to the controls, indicating that the NPs effectively inhibit tumor angiogenesis cell proliferation and induce apoptosis.[27] The recently developed, representative, "smart" biocompatible NG systems and the synthesis routes of various therapeutic and diagnostic applications are listed in Table 1.

https://dx.doi.org/10.1021/acsomega.0c05276
ACS Omega 2021, 6, 5075−5090

4. NANOGELS: THE CLINICAL STATUS AND TRANSLATIONAL CHALLENGES

Recently, smart NGs emerged as a promising system for various biomedical domains, majorly in pharmaceutical delivery and biomedical diagnostics. However, to date, only a few NG systems have been entered into clinical investigations. Recently, polysaccharide-based self-assembled NGs have been witnessed to incorporate therapeutic molecules, resulting in the construction of cancer and nasal vaccines, and cytokine or gene delivery systems were recently reviewed by Tahara and Akiyoshi.[38] After preclinical investigations, some NG systems were moved to phase I clinical investigations, and it was realized that formulations are safe for repeated use in humans and do not induce any harmful side effects. Notably, only the cholesterol−pullulan protein-delivery NG system was attempted in trials (Phase 1) as intranasal vaccines, as the HER-2 antigen carrier toward tumor therapy, and also to transport the NY-ESO-1 antigen against melanoma and esophageal tumors.

Even though NGs have been successfully employed in many biomedical applications ranging from drug delivery, diagnostics, and imaging, there are several hurdles that still exist that need to be overcome for successful clinical translation. Recently, Bronich and colleagues detailed the clinical studies and major hurdles toward clinical translation of NGs in an excellent review.[39] In a brief outlook, the main disadvantage of NGs is the rapid systemic clearance through the kidney, liver, spleen, etc. after the administration. Notably, the biodistribution of the NGs was influenced by several factors like size, shape, surface charge, composition, and type of theranostic encapsulated. The possible fast clearance though the spleen as well as the kidney indicates that the size and shape of the NG have to be better defined to achieve prolonged blood circulation. The opsonization of NGs by serum proteins might influence the circulation half-life, and the NG charge can also alter the opsonization profile. It was identified that NGs with an almost neutral surface charge displayed an extended circulation. However, the most necessary feature, stimuli-responsiveness, generally arises from charged functionalities of the network, and such functionalities are necessary to facilitate encapsulation and hold the theranostic cargo. Thus, it is challenging to achieve the delicate balance among charge-related responsive characteristics by avoiding other nonspecific interactions during *in vivo* scenarios.[39]

Notable challenges exist in delivering biomolecules, for example, nonviral gene and therapeutic proteins through NGs. In nucleic acid delivery, the major drawback is the low efficiency relative to viral vectors, due to the genetic material degradation in the intracellular level, and it is challenging to design a delivery system which facilitates an effective endosomal release of the carrier. In a protein release scenario, since the proteins are highly sensitive to various steps during the formulation process, the selection of the NG and the identification of ideal formulation parameters are critical to preserve protein structure and function. Besides, most of the stimuli-responsive NGs underwent degradation at the target site, and therefore, the simultaneous control of both stimuli-triggered therapeutic delivery as well as degradation kinetics is difficult.[39] Conclusively, addressing the obstacles related to scalable, reproducible NG synthesis is critical, and the complexity as well as diverse structural and functional characteristics demands careful design to achieve an expected therapeutic outcome.

5. CONCLUSIONS AND OUTLOOK

In recent years, significant research effort has been invested toward the construction of "smart" NGs through various synthesis approaches such as free radical, RAFT, ATRP, and NCA ring-opening polymerizations and emulsion techniques. The "smart" NGs demonstrated biocompatibility and the ability to be a cargo for various pharmaceutical/diagnostic agents, with excellent programmed release capabilities, triggered by different stimuli-responsiveness. Herein, we have outlined the representative synthesis strategies of various "smart" NGs and notable applications of targeted drug/gene delivery, PDT and PTT, biosensing, as well as imaging. Even though to date plenty of studies are available, the *in vivo* studies of NGs in various biomedical domains are comparably less. Conclusively, the application of most of these NGs is still on the way to clinical applications. It is important that the developed NGs have to pass through various clinical stages, and efforts are needed for satisfactory clinical results, especially regarding the *in vivo* safety and efficacy of the NGs for bench to bedside transformation.

AUTHOR INFORMATION

Corresponding Author

Renjith P. Johnson − *Polymer Nanobiomaterial Research Laboratory, Nanoscience and Microfluidics Division, Yenepoya Research Centre, Yenepoya (Deemed to be University), Mangalore, Karnataka 575018, India;* orcid.org/0000-0002-2222-2515; Phone: +91 8242204669; Email: renjithjohnson@yenepoya.edu.in

Authors

Namitha K. Preman − *Polymer Nanobiomaterial Research Laboratory, Nanoscience and Microfluidics Division, Yenepoya Research Centre, Yenepoya (Deemed to be University), Mangalore, Karnataka 575018, India*

Supriya Jain − *Polymer Nanobiomaterial Research Laboratory, Nanoscience and Microfluidics Division, Yenepoya Research Centre, Yenepoya (Deemed to be University), Mangalore, Karnataka 575018, India*

Complete contact information is available at: https://pubs.acs.org/10.1021/acsomega.0c05276

Author Contributions

†N.K.P. and S.J. contributed equally to the manuscript.

Notes

The authors declare no competing financial interest.

Biographies

https://dx.doi.org/10.1021/acsomega.0c05276
ACS Omega 2021, 6, 5075−5090

Namitha K. Preman has been a Ph.D. candidate since 2017 under the supervision of Dr. Renjith P. Johnson at Polymer Nanobiomaterial Research Laboratory, Nanoscience and Microfluidics Division, Yenepoya Research Center, Yenepoya (Deemed to be University), India. She received her B.Sc degree (2014) in Chemistry from Kannur University and M.Sc. degree in Biopolymer Science from Cochin University of Science and Technology in 2016. She is a recipient of a Senior Research Fellowship from the Indian Council of Medical Research (ICMR), Govt. of India. Her research interests are focused on development of stimuli-responsive polymer gels and prodrugs for wound healing, drug delivery, and sensing applications.

Supriya Jain has been a Ph.D. candidate since 2018 under the supervision of Dr. Renjith P. Johnson at Polymer Nanobiomaterial Research Laboratory, Nanoscience and Microfluidics Division, Yenepoya Research Center, Yenepoya (Deemed to be University), India. She received her M.Sc. degree in Analytical Chemistry from St. Aloysius College (Affiliated to Mangalore University) India in 2018. Currently, she is working as a Junior Research Fellow on the Core Research Grant from Department of Science and Technology-Science and Engineering Research Board (DST-SERB), Govt. of India. Her research interests are focused on the development of conducting polymer-based hybrid materials for biomedical applications.

Dr. Renjith P. Johnson is an Assistant Professor in the Nanoscience and Microfluidics Division, Yenepoya Research Center (YRC), Yenepoya (Deemed to be University), India. In 2014, he earned his Ph.D. (Polymer Science and Engineering) in the laboratory of Prof. Il Kim at Pusan National University (PNU), Republic of Korea. He completed his postdoctoral training at PNU and at the University of South Carolina, USA, in the laboratory of Prof. Peisheng Xu. Since returning to Yenepoya (Deemed to be University) in 2016, he has been the head of the Polymer Nanobiomaterials Research Laboratory at YRC. He received research grants from National Funding Agencies (Department of Science and Technology-Science and Engineering Research Board, Department of Biotechnology, and Biotechnology Industry Research Assistance Council) as a Principal Investigator and Co-Investigator for executing various projects. He has developed novel products/technologies and, to date, has four patent applications under process. His research interests are mainly focused on polymer synthesis, nanomedicine, and development of novel polymeric scaffolds for tissue engineering applications.

■ ACKNOWLEDGMENTS

This work was supported by Core Research Grant (CRG/2018/000380−2019) from the Department of Science and Technology-Science and Engineering Research Board (DST-SERB), Govt. of India, and the Indian Council of Medical Research (2019-5984), Govt. of India.

■ ABBREVIATIONS:

AA, acrylic acid; AMF, alternative magnetic field; ATRP, atom transfer radical polymerization; BSA, bovine serum albumin; CLSM, confocal laser scanning microscopy; DEX, dexamethasone; DMSO, dimethyl sulfoxide; Dox, doxorubicin; DLC, drug loading content; DLE, drug loading efficiency; DLS, dynamic light scattering; EGFR, epidermal growth factor receptor; EDC/NHS, ethyl dicyclohexylcarbodiimide/*N*-hydroxysuccinimide; EGDMA, ethylene glycol dimethacrylate; FRET, Forster resonance energy transfer; FMT, fluorescence molecular tomography; GSH, glutathione; R_h, hydrodynamic diameter; HA, hyaluronic acid; HEMA, 2-hydroxyethyl methacrylate; ICG, indocyanine green; IBD, inflammatory bowel diseases; LBL, layer-by-layer; LCST, lower critical solution temperature; MRI, magnetic resonance imaging; MMP, matrix metalloproteinases; MAA, methacrylic acid; MTX, methotrexate; ND, nanodiamond; NGs, nanogels; NCA, *N*-carboxy-anhydrides; NIR, near infrared; BIS, *N*,*N*-methylene-bis-(acrylamide); MBA, *N*,*N*-methylene bisacrylamide; BAC, *N*,*N*′-bis(acryloyl) cystamine; NIPAM, *N*-isopropylacrylamide; DHPMA, *N*-(1,3-dihydroxypropan-2-yl) methacrylamide; NTA, nitrilotriacetic acid; OEGMA, oligo(ethylene glycol) methacrylate; OEGDA, oligo(ethylene glycol) diacrylate; PBA, phenylboronic acid; PTT, photothermal therapy; PDT, photodynamic therapy; PNVCL, poly(*N*-vinyl caprolactam); PET, positron emission tomography; PEI, polyethylenimine; PPS, potassium persulfate; PPY, polypyrrole; PPa, pyro pheophorbide-a; RAFT, reversible addition−fragmentation chain transfer; RHB, rhodamine; ROP, ring-opening polymerization; SDS, sodium dodecyl sulfate; SBMA, sulfobetaine methacrylate; siRNA, small interfering ribonucleic acid; TPP, tetraphenylporphyrin; TM, timolol maleate; TEM, transmission electron microscope; MPS, 3-(trimethoxysilyl) propyl methacrylate; UV, ultraviolet; VPTT, volume phase temperature transition

■ REFERENCES

(1) Ramos, J.; Forcada, J.; Hidalgo-Alvarez, R. Cationic Polymer Nanoparticles and Nanogels: from Synthesis to Biotechnological Applications. *Chem. Rev.* **2014**, *114*, 367−428.

(2) Kabanov, A.-V.; Vinogradov, S.-V. Nanogels as Pharmaceutical Carriers: Finite Networks of Infinite Capabilities. *Angew. Chem., Int. Ed.* **2009**, *48*, 5418−5429.

(3) Sanson, N.; Rieger, J. Synthesis of Nanogels/microgels by Conventional and Controlled Radical Crosslinking Copolymerization. *Polym. Chem.* **2010**, *1*, 965−977.

(4) Hajebi, S.; Abdollahi, A.; Roghani-Mamaqani, H.; Salami-Kalajahi, M. Temperatureresponsive poly(*N*-isopropylacrylamide) Nanogels: The Role of Hollow Cavities and Different Shell Cross-linking

https://dx.doi.org/10.1021/acsomega.0c05276
ACS Omega 2021, 6, 5075−5090

Densities on Doxorubicin Loading and Release. *Langmuir* **2020**, *36*, 2683−2694.
(5) Molina, M.; Asadian-Birjand, M.; Balach, J.; Bergueiro, J.; Miceli, E.; Calderón, M. Stimuli-responsive Nanogel Composites and Their Application in Nanomedicine. *Chem. Soc. Rev.* **2015**, *44*, 6161−6186.
(6) Wu, H.-Q.; Wang, C. C. Biodegradable Smart Nanogels: A New Platform for Targeting Drug Delivery and Biomedical Diagnostics. *Langmuir* **2016**, *32*, 6211−6225.
(7) Li, Y.; Maciel, D.; Rodrigues, J.; Shi, X.; Tomas, H. Biodegradable polymer nanogels for drug/nucleic acid delivery. *Chem. Rev.* **2015**, *115*, 8564−8608.
(8) Hajebi, S.; Rabiee, N.; Bagherzadeh, M.; Ahmadi, S.; Rabiee, M.; Roghani-Mamaqani, H.; Tahriri, M.; Tayebi, L.; Hamblin, M. R. Stimulus-responsive polymeric nanogels as smart drug delivery systems. *Acta Biomater.* **2019**, *92*, 1−8.
(9) Ekkelenkamp, A. E.; Elzes, M. R.; Engbersen, J. F.; Paulusse, J. M. Responsive crosslinked polymer nanogels for imaging and therapeutics delivery. *J. Mater. Chem. B* **2018**, *6*, 210−235.
(10) Su, S.; Wang, H.; Liu, X.; Wu, Y.; Nie, G. iRGD-coupled Responsive Fluorescent Nanogel for Targeted Drug Delivery. *Biomaterials* **2013**, *34*, 3523−3533.
(11) Ahmed, M.; Wattanaarsakit, P.; Narain, R. Cationic glyconanogels for Epidermal Growth Factor Receptor (EGFR) Specific siRNA Delivery in Ovarian Cancer Cells. *Polym. Chem.* **2013**, *4*, 3829−3836.
(12) Knipe, J.-M.; Strong, L.-E.; Peppas, N.-A. Enzyme-and pH-responsive Microencapsulated Nanogels for Oral Delivery of siRNA to induce TNF-α Knockdown in the Intestine. *Biomacromolecules* **2016**, *17*, 788−797.
(13) Xing, T.; Mao, C.; Lai, B.; Yan, L. Synthesis of Disulfide-crosslinked Polypeptide Nanogel Conjugated with a Near-infrared Fluorescence Probe for Direct Imaging of Reduction-induced Drug Release. *ACS Appl. Mater. Interfaces* **2012**, *4*, 5662−5672.
(14) Cazares-Cortes, E.; Espinosa, A.; Guigner, J.-M.; Michel, A.; Griffete, N.; Wilhelm, C.; Ménager, C. Doxorubicin Intracellular Remote Release from Biocompatible Oligo(ethylene glycol) Methyl Ether Methacrylate-based Magnetic Nanogels Triggered by Magnetic Hyperthermia. *ACS Appl. Mater. Interfaces* **2017**, *9*, 25775−25788.
(15) Li, F.; Yang, H.; Bie, N.; Xu, Q.; Yong, T.; Wang, Q.; Gan, L.; Yang, X. Zwitterionic Temperature/redox-sensitive Nanogels for Near-infrared Light-triggered Synergistic Thermo-Chemotherapy. *ACS Appl. Mater. Interfaces* **2017**, *9*, 23564−23573.
(16) Kim, H.-J.; Zhang, K.; Moore, L.; Ho, D. Diamond Nanogel-embedded Contact Lenses Mediate Lysozyme-dependent Therapeutic Release. *ACS Nano* **2014**, *8*, 2998−3005.
(17) Chen, S.; Bian, Q.; Wang, P.; Zheng, X.; Lv, L.; Dang, Z.; Wang, G. Photo, pH and Redox Multi-responsive Nanogels for Drug Delivery and Fluorescence Cell Imaging. *Polym. Chem.* **2017**, *8*, 6150−6157.
(18) Theune, L.-E.; Buchmann, J.; Wedepohl, S.; Molina, M.; Laufer, J.; Calderón, M. NIR and Thermo-responsive Semi-interpenetrated Polypyrrole Nanogels for Imaging Guided Combinational Photothermal and Chemotherapy. *J. Controlled Release* **2019**, *311*, 147−161.
(19) Yao, X.; Chen, L.; Chen, X.; Xie, Z.; Ding, J.; He, C.; Zhang, J.; Chen, X. pH-responsive Metallo-Supramolecular Nanogel for Synergistic Chemo-photodynamic Therapy. *Acta Biomater.* **2015**, *25*, 162−171.
(20) Hang, C.; Zou, Y.; Zhong, Y.; Zhong, Z.; Meng, F. NIR and UV-responsive Degradable Hyaluronic acid Nanogels for CD44$^-$targeted and Remotely Triggered Intracellular Doxorubicin delivery. *Colloids Surf., B* **2017**, *158*, 547−555.
(21) Li, C.; Wu, G.; Ma, R.; Liu, Y.; Liu, Y.; Lv, J.; An, Y.; Shi, L. Nitrilotriacetic acid (NTA) and Phenylboronic acid (PBA) Functionalized Nanogels for Efficient Encapsulation and Controlled Release of Insulin. *ACS Biomater. Sci. Eng.* **2018**, *4*, 2007−2017.
(22) Don, T.-M.; Lu, K.-Y.; Lin, L.-J.; Hsu, C.-H.; Wu, J.-Y.; Mi, F.-L. Temperature/pH/Enzyme Triple-responsive Cationic Protein/PAA-b-PNIPAAm Nanogels for Controlled Anticancer Drug and Photosensitizer Delivery Against Multidrug Resistant Breast Cancer Cells. *Mol. Pharmaceutics* **2017**, *14*, 4648−4660.
(23) Massi, L.; Najer, A.; Chapman, R.; Spicer, C. D.; Nele, V.; Che, J.; Booth, M.-A.; Doutch, J.-J.; Stevens, M.-M. Tuneable Peptide Cross-linked Nanogels for Enzyme-triggered Protein Delivery. *J. Mater. Chem. B* **2020**, *8*, 8894−8907.
(24) Farazi, S.; Chen, F.; Foster, H.; Boquiren, R.; McAlpine, S.-R.; Chapman, R. Real Time Monitoring of Peptide Delivery In Vitro Using High Payload pH Responsive Nanogels. *Polym. Chem.* **2020**, *11*, 425−432.
(25) Zhang, Y.; Zhang, J.; Xing, C.; Zhang, M.; Wang, L.; Zhao, H. Protein Nanogels with Temperature-induced Reversible Structures and Redox Responsiveness. *ACS Biomater. Sci. Eng.* **2016**, *2*, 2266−2275.
(26) Chen, K.; Liao, S.; Guo, S.; Zheng, X.; Wang, B.; Duan, Z.; Zhang, H.; Gong, Q.; Luo, K. Multistimuli-responsive PEGylated polymeric bioconjugate-based nano-aggregate for cancer therapy. *Chem. Eng. J.* **2020**, *391*, 123543.
(27) Cai, H.; Dai, X.; Wang, X.; Tan, P.; Gu, L.; Luo, Q.; Zheng, X.; Li, Z.; Zhu, H.; Zhang, H.; Gu, Z.; Gong, Q.; Luo, K. A Nano-strategy for Efficient Imaging-Guided Antitumor Therapy through a Stimuli-Responsive Branched Polymeric Prodrug. *Adv. Sci.* **2020**, *7*, 1903243.
(28) Ding, J.; Shi, F.; Li, D.; Chen, L.; Zhuang, X.; Chen, X. Enhanced Endocytosis of Acid- Sensitive Doxorubicin Derivatives with Intelligent Nanogel for Improved Security and Efficacy. *Biomater. Sci.* **2013**, *1*, 633−646.
(29) Zou, Y.; Li, D.; Wang, Y.; Ouyang, Z.; Peng, Y.; Tomás, H.; Xia, J.; Rodrigues, J.; Shen, M.; Shi, X. Polyethylenimine Nanogels Incorporated with Ultrasmall Iron Oxide Nanoparticles and Doxorubicin for MR Imaging-Guided Chemotherapy of Tumors. *Bioconjugate Chem.* **2020**, *31*, 907−915.
(30) Gao, F.; Wu, X.; Wu, D.; Yu, J.; Yao, J.; Qi, Q.; Cao, Z.; Cui, Q.; Mi, Y. Preparation of Degradable Magnetic Temperature-and Redox-Responsive Polymeric/Fe_3O_4 Nanocomposite Nanogels in Inverse miniemulsions for Loading and Release of 5- fluorouracil. *Colloids Surf., A* **2020**, *587*, 124363.
(31) Zhang, Y.; Dosta, P.; Conde, J.; Oliva, N.; Wang, M.; Artzi, N. Prolonged Local In Vivo Delivery of Stimuli-Responsive Nanogels That Rapidly Release Doxorubicin in Triple-Negative Breast Cancer Cells. *Adv. Healthcare Mater.* **2020**, *9*, 1901101.
(32) Cao, Y.; Mao, Z.; He, Y.; Kuang, Y.; Liu, M.; Zhou, Y.; Zhang, Y.; Pei, R. Extremely Small Iron Oxide Nanoparticles-Encapsulated Nanogels as a Glutathione-Responsive T1 Contrast Agent for Tumor-Targeted Magnetic Resonance Imaging. *ACS Appl. Mater. Interfaces* **2020**, *12*, 26973−26981.
(33) Li, Z.; Van Zee, N. J.; Bates, F. S.; Lodge, T. P. Polymer Nanogels as Reservoirs To Inhibit Hydrophobic Drug Crystallization. *ACS Nano* **2019**, *13*, 1232−1243.
(34) Gao, L.; Zabihi, F.; Ehrmann, S.; Hedtrich, S.; Haag, R. Supramolecular nanogels fabricated via host−guest molecular recognition as penetration enhancer for dermal drug delivery. *J. Controlled Release* **2019**, *300*, 64−72.
(35) Zhang, X.; Wu, Y.; Li, Z.; Wang, W.; Wu, Y.; Pan, D.; Gu, Z.; Sheng, R.; Tomas, H.; Zhang, H.; Rodrigues, J.; Gong, Q.; Luo, K. Glycodendron/pyropheophorbide-a (Ppa)-functionalized HA as a nanosystem for tumor photodynamic therapy. *Carbohydr. Polym.* **2020**, *247*, 116749.
(36) Gordon, M. R.; Zhuang, J.; Ventura, J.; Li, L.; Raghupathi, K.; Thayumanavan, S. Biodistribution Analysis of NIR-labeled Nanogels Using In Vivo FMT Imaging in Triple Negative Human Mammary Carcinoma Models. *Mol. Pharmaceutics* **2018**, *15*, 1180−1191.
(37) Wu, W.; Mitra, N.; Yan, E. C.; Zhou, S. Multifunctional Hybrid Nanogel for Integration of Optical Glucose Sensing and Self-regulated Insulin Release at Physiological pH. *ACS Nano* **2010**, *4*, 4831−4839.
(38) Tahara, Y.; Akiyoshi, K. Current Advances in Self-assembled Nanogel Delivery Systems for Immunotherapy. *Adv. Drug Delivery Rev.* **2015**, *95*, 65−76.
(39) Soni, K. S.; Desale, S. S.; Bronich, T. K. Nanogels: An Overview of Properties, Biomedical Applications and Obstacles to Clinical Translation. *J. Controlled Release* **2016**, *240*, 109−126.

https://dx.doi.org/10.1021/acsomega.0c05276
ACS Omega 2021, 6, 5075−5090